이학박사 학위논문

The AT-hook motif-containing protein AHL22 regulates flowering initiation by modifying *FLOWERING LOCUS T* chromatin in *Arabidopsis*

AT-hook motif를 포함한 AHL22 protein의 *FT* chromatin 변형을 통한 개화 시기 조절

2014년 2월

서울대학교 대학원

화학부

윤 주

The AT-hook motif-containing protein AHL22 regulates flowering initiation by modifying *FLOWERING LOCUS T* chromatin in *Arabidopsis*

AT-hook motif를 포함한 AHL22 protein의
FT chromatin 변형을 통한 개화 시기 조절

지도교수 박 충 모

이 논문을 이학박사학위논문으로 제출함

2013년 11월

서울대학교 대학원

화학부

윤 주

윤주의 박사학위 논문을 인준함

2013년 12월

위 원 장 _____ (인)

부위원장 _____ (인)

위 원 _____ (인)

위 원 _____ (인)

위 원 _____ (인)

ABSTRACT

Coordination of the onset of flowering with developmental status and seasonal cues is critical for reproductive success in plants. Molecular genetic studies on *Arabidopsis* mutants that have alterations in flowering time have identified a wide array of genes that belong to distinct genetic flowering pathways. The flowering time genes are regulated through versatile molecular and biochemical mechanisms, such as controlled RNA metabolism and chromatin modifications. Recent studies have shown that a group of AT-hook DNA-binding motif-containing proteins plays a role in plant developmental processes and stress responses.

Here, I demonstrate that the AT-hook protein AHL22 (AT-hook motif nuclear localized 22) regulates flowering time by modifying *FLOWERING LOCUS T* (*FT*) chromatin in *Arabidopsis*. I showed that *AHL22* and *FT* are expressed together in leaf vascular tissues and that AHL22 represses *FT* expression throughout development. AHL22 binds to a stretch of AT-rich sequence in the *FT* locus. AHL22 interacts with a subset of histone deacetylases. An *Arabidopsis* mutant overexpressing the *AHL22* gene (OE-*AHL22*) exhibited delayed flowering, and *FT* transcription was significantly reduced in the mutant.

Consistent with the delayed flowering and *FT* suppression in the OE *AHL22* mutant, histone 3 (H3) acetylation was reduced and H3 lysine 9 dimethylation was elevated in the *FT* chromatin.

I propose that AHL22 acts as a chromatin chromatin remodeling factor that modifies the architecture of *FT* chromatin by modulating both H3 acetylation and methylation.

Key words : *Arabidopsis* · flowering time · AT-hook DNA binding protein · AT-rich sequence · *FT* · chromatin

Student Number : 2003-30870

CONTENTS

LIST OF FIGURES

LIST OF TABLES

ABBREVIATIONS

AHL22	AT-hook motif nuclear localized 22
ATR	AT-rich sequence
BiFC	Biomolecular fluorescence complementation
CaMV	Cauliflower mosaic virus
cFT	cDNA FT
DIC	Differential interference contrast microscopy
EMSA	Electrophoretic mobility shift assay
ESC	ESCAROLA
FLC	FLOWERING LOCUS C
FRI	FRIGIDA
FT	FLOWERING LOCUS T
gFT	Genomic FT
GUS	*β*-Gucuronidase
H3	Histone 3
H3Ac	H3 acetylation
H3K27me3	H3 trimethylation at Lys-27
H3K9me2	H3 dimethylation at Lys-9

HDAC	Histone deacetylase
LD	Long day
LFY	LEAFY
MAR	Matrix attachment region
MBP	Maltose binding protein
MS	Murashige & Skoog
qRT-PCR	Quantitative real-time RT-PCR
RLN	Rosette leaf number
SOC1	SUPPRESSOR of OVEREXPRESSION of CONSTANS1
TEM1	TEMPRANILLO
TSA	Trichostatin A
YFP	Yellow fluorescent protein

I. BACKGROUND

1.1. Flowering time control in *Arabidopsis*

Arabidopsis thaliana is a small flowering plant that is one of the most studied model organism in plant biology. It has been used in physiological and genetic researches for a variety of mutant screening to elucidate molecular mechanism of flowering process during the past decades. The DNA sequencing of *Arabidopsis* Col-0 genome has been determined in 2000 (Arabidopsis Genome Initiative 2000), founded containing about 25,500 genes encoding proteins of genome. As the genome sequence has facilitated, extensive characterization from various mutant-screening processes and isolating mutants of interest have made *Arabidopsis* a useful model for genetic analysis of floral transition.

The floral transition from vegetative to reproductive state is a major developmental change in the plant life cycle and must be properly timed to maximize reproductive success. During this transition, the shoot apical meristem (SAM) undergoes a change in fate from vegetative meristem producing leaf primodia to inflorescence meristem producing flowers. The flowering of plants is regulated by various environmental stimuli and endogenous developmental factors. Environmental signals from day-length change, prolonged low temperature exposure and ambient temperature

fluctuation, together with responding to endogenous factors such as age and plant hormone gibberellins, form an integrated regulatory network to control the timing of flower initiation under a given environment (Figure 1).

Photoperiodism is the physiological responses to changes in the relative length of day and night, while vernalizaion is a process that requires for many plants to undergo a period of low temperature to initiate or accelerate the flowering and is different from cold acclimation process which shows rapid response to cold (Thomashow, 2001).

The respond to day length (photoperiod) is diverse among species according to their habits. Some plants flower earlier when the day is shorter than a critical length of time, while others flower faster when the day is longer. *Arabidopsis* is a facultative long-day plant, flowering earlier under long days (LD) than short days (SD). Several late flowering mutants have been reported to defective in photoperiod pathway. The mutation in photoperiod pathway genes cause late flowering in inductive long days, but do not affect on flowering time in non-inductive short days.

The autonomous (age dependent) pathway mutants also exhibited late flowering, but are differed from photoperiod pathway mutants because they flower later in SD than in LD, which indicates that these mutants distinguish the day-length difference (Simpson et al., 2003).

Gibberellins promote flowering in *Arabidopsis* and are absolutely required for flowering under SD conditions, because GA signaling mutants and GA biosynthesis mutants seldom flower in SD (Reeves and Coupland, 2001).

Small changes in ambient temperature also affect flowering time. Exposure to low ambient temperatures (16℃) delays flowering compared to warm growth temperatures of 20~24℃ regardless of day length and exposure to high ratios of far-red to red light promotes flowering related to shading conditions (Blázquez et al., 2003; Cerdan and Chory, 2003).

1.2. Genetic flowering pathway in *Arabidopsis*

Many flowering-time mutations have been identified in *Arabidopsis*. These mutations affect genes that are involved in responses to environmental stimuli and endogenous developmental state of flowering. Two approaches have been used to identify genes that are involved in the genetics of the transition to flowering. The first utilizes the analysis of natural variation in flowering-time control occurring between different ecotypes of *Arabidopsis*, and the second method utilizes isolation of flowering-time mutants via mutagenesis. This genetic analysis of *Arabidopsis* mutants and ecotypes led to the identification of four major flowering-time genetic pathways: photoperiod (day length perception), vernalization (temperature), gibberellin and autonomous

(developmental ages) (Mouradov et al., 2002; Simpson and Dean, 2002). In addition to these four main pathways, the ambient temperature also affects the flowering of *Arabidopsis* (Blázquez et al., 2003) (Figure 1).

Physiological and molecular genetic analyses of late and early flowering mutants of Arabidopsis have identified several genes involved in flowering finally increase the expression levels downstream target genes. The common target genes are called flowering time integrators, such as *FT*, *SUPPRESSOR OF OVEREXPRESSION OF CONSTANS1* (*SOC1*)/*AGAMOUS - LIKE20* (*AGL20*), and *LEAFY* (*LFY*) (Blázquez and Weigel, 2000; Lee et al., 2000; Samach et al., 2000). Their expression is regulated by two antagonistic flowering regulators CONSTANS (CO) and FLOWERING LOCUS C (FLC) which act as floral activator and repressor, respectively.

GIGANTEA (*GI*) and *CONSTANS* (*CO*) are important genes in photoperiod pathway. *GI* controls circadian rhythms and flowering time and acts earlier in the hierarchy than *CO* and *FT* (Mizoguchi et al., 2005). CO induces the transcription of floral integrators, *FT* and *SOC1* (Suarez-Lopez et al., 2001; Yanovsky and Kay, 2002). In young plants, *CO* and *FT* are expressed in phloem companion cells, particularly in those of the distal minor veins of leaves (An et al., 2004; Takada and Goto, 2003). *CO* mRNA is expressed in the shoot apical region above the protophloem, but CO protein is restricted to the phloem companion cells (Simon et al., 1996; An et al., 2004).

Ectopic expression of *CO* using heterologous promoters and grafting experiments placed CO upstream of a leaf-borne mobile signal. In contrast, expression of *CO* in the SAM does not stimulate flowering (An et al., 2004). On the contrary, *FT* promotes early flowering when expressed in the leaf phloem or the SAM, and expression of *FT* in either of these tissues induces the floral transition even in the lack of functional *CO* (An et al., 2004). These experiments indicate that *CO* expression only in the leaves might be sufficient to generate a mobile signal for flowering induction and *CO* acts upstream in the signaling pathway of *FT*. Although FT mRNA is expressed only in the veins of leaves (Takada and Goto, 2003), FT protein functions in the meristem, where it induces the expression of the meristem identity genes (Abe et al., 2005; Wigge et al., 2005). Therefore, the spatial pattern of *FT* mRNA expression and FT protein location acts given evidence that a product of FT show the mobile signal. (An et al., 2004; Turck et al., 2008)

The autonomous and the vernalization pathways independently regulate the floral transition by repressing *FLOWERING LOCUS C* (*FLC*) expression. (Hepworth et al., 2002). It has been shown that FLC represses the expression of floral integrators, *FT* and *SOC1* by binding to their *cis*-elements (Searle et al., 2006). In addition, GAs mediated signals appear to activate directly the floral integrators *SOC1*, *LFY*, and probably *FT* (Blázquez et al., 1998; Moon et al., 2003).

Among these flowering pathway integrator genes, *FT* has a central role in flowering promotion and functions, because multiple flowering pathways, including the long-day, vernalization, autonomous pathways, are integrated into the regulation of *FT* expression. *FT* expression is mainly regulated by ambient temperature of thermosensory pathway, independently of the photoperiod pathway, to regulate flowering time (Balasubramanian et al., 2006; Blázquez et al., 2003).

Under ambient temperature conditions (for example, 16℃), decreased *FT* expression causes late flowering (Lee et al., 2007), whereas growth temperature rises (for example, 17 to 27 ℃) upregulate the expression of bHLH transcription factor *PHYTOCHROME INTERACTING FACTOR 4* (*PIF4*) at directly activates *FT* expression to promote flowering (Kumar et al., 2012).

Furthermore, loss-of-function *ft* mutations cause a severe late flowering phenotype, and overexpression of *FT* causes an early flowering phenotype that is independent of day length and temperature (Kardailsky et al., 1999; Kobayashi et al., 1999; Blázquez et al., 2003). The FT protein moves from leaf (phloem companion cells) to the shoot apical meristem, where it subsequently forms a complex with the bZIP transcriptional factor FD to activate the expression of floral-meristem identity genes *LFY* and *APETALA1* (*AP1*), leading to floral primordium formation (Abe et al., 2005; Wigge et al., 2005).

1.3. The regulation of flowering by chromatin-based mechanisms

Chromatin modifications mediate the regulation of developmental genes in plants. These modifications, including nucleosome remodeling, histone modifications and DNA methylation, can alter the chromatin structure and gene expression. In general, active gene expression is associated with histone acetylation, histone H3 lysine-4 trimethylation (H3K4me3), H2B mono-ubiquitination (H2Bub1), and H3 lysine-36 di- and trimethylation (H3K36me2/me3), whereas gene repression is linked with histone deacetylation, H3 lysine-9 methylation, H3 lysine-27 trimethylation (H3K27me3), and H2A monoubiquitination (H2Aub1) (He, 2012).

In *Arabidopsis* research, expression of *FLC* and *FT*, two central regulators of flowering, is regulated by diverse chromatin modifications to regulate flowering time. Chromatin modification of the floral repressor *FLC* has been the best studied. For instance, the *ARABIDOPSIS TRITHORAX1* (*ATX1*) H3K4 methyltransferase and the *EARLY FLOWERING IN SHORT DAYS* (*EFS*) H3K36 methyltransferase mediate H3K4 and H3K36 methylation on *FLC* chromatin, respectively; both are elevated *FLC* expression (Pien et al., 2008; Xu et al.,2008).

In addition, H2Bmono-ubiquitination (Cao et al., 2008; Gu et al., 2009), deposition of the histone variant H2A.Z (Deal et al., 2007; Zilberman et al., 2008) and *FLC* regulation by FRIGIDA (FRI) (Choi et al., 2011), a

plant-specific scaffold protein, is part of a complex recruiting chromatin modifiers to the *FLC* locus as active marks for *FLC* transcription.

In contrast, histone deacetylation (Austin et al., 2004; He et al., 2003), H3K4 demethylation (Jiang et al., 2007; Liu et al., 2007b), histone H3K9 tri-methylation (Liu et al., 2004; Swiezewski et al., 2007), H3K27 tri-methylation (Jiang et al., 2008), and H4R3 symmetric di-methylation (H4R3sme2) (Wang et al., 2007) repress *FLC* transcription.

Vernalization is a process that suppresses *FLC* expression through distinct histone modifications in the *FLC* chromatin, including H3K9 and H3K27 di- and tri-methylation, H4R3sme2, histone deacetylation, and H3K4 demethylation (Bastowet al., 2004; Finnegan and Dennis, 2007; Greb et al., 2007; Schmitz et al., 2008; Sung and Amasino, 2004; Sung et al., 2006). Therefore, *FLC* chromatin undergoes distinct modifications in response to endogenous developmental and environmental signals.

Also, Chromatin modifications play an important role in the regulation of *FT* expression. *FT* is a major flowering time integrator that induced in the vasculature by a long-day photoperiod and ambient temperature rise. While histone modifications have been studied extensively in *FLC* chromatin, relatively little is known about the histone modification of *FT* chromatin. Recent studies show that diverse chromatin modifiers are associated with regulation of *FT* expression, including Polycomb Repressive

Complex2 (PRC2), LIKE HETEROCHROMATIN PROTEIN 1 (LHP1), RELATIVE OF EARLY FLOWERING 6 (REF6), *Arabidopsis thaliana* JUMONJI4 (AtJMJ4), and ACTIN-RELATED PROTEIN 6 (ARP6) (He, 2012).

It is likely that PRC2 functions *in vivo* primarily as a methyl-transferase acting on lysine 27 of histone H3 (H3K27). In *Arabidopsis*, CURLY LEAF (CLF), a putative H3K27 methyltransferase and a component of PRC2 complexes, binds to *FT* chromatin and mediates the deposition of H3K27me3 in *FT* chromatin and *FT* repression (Jiang et al., 2008). Other PRC2 components, including SWINGER (SWN), EMBRYONIC FLOWER 2 (EMF2), and FERTILIZATION INDEPENDENT ENDOSPERM (FIE) also repress *FT* expression (Jiang et al., 2008; Farrona et al., 2011), suggesting that a PRC2 like complex deposits H3K27me3 at *FT* chromatin to repress its expression in the vasculature (He, 2012).

H3K27me3 is actively removed by H3K27 demethylases. A recent study has revealed that REF6, also known as Jumonji domain–containing protein 12 (JMJ12), specifically demethylates H3K27me3 and contributes to gene activation by removing repressive H3K27me3 marks (Lu et al., 2011).

LHP1/TERMINAL FLOWER 2 (TFL2), the *Arabidopsis* homologue of HETEROCHROMATIN PROTEIN 1 (HP1), recognizes H3K27me3 and binds directly to *FT* chromatin to repress *FT* expression in the vasculature (Turck et al., 2007). Therefore, the levels of H3K27me3 at *FT* are dynamically

regulated by the PRC2 and REF6 (He, 2012). In addition, another putative PRC1-like component called EMBRYONIC FLOWER 1 (EMF1), acts in cooperation with the PRC2 to repress *FT* expression and eventually inhibit flowering (Moon et al., 2003; Bratzel et al., 2010). *FT* chromatin has simultaneously bivalent chromatin marks of active H3K4me3 and repressive H3K27me3, with H3K27me3 being prevalent in young *Arabidopsis* seedlings in which *FT* is expressed at a low level (Jiang et al., 2008). Loss of PRC2 mediated H3K27me3 function leads to increase of H3K4me3 in *FT* (Jiang et al., 2008).

Recent studies have revealed that methylated H3K4 demethylase AtJMJ4 associate directly with *FT* chromatin and mediates H3K4 demethylation at *FT* to repress its expression (Jeong et al., 2009; Yang et al., 2010; Lu et al., 2010). Loss of AtJMJ4 function leads to an increase in H3K4me3 and a reduction in H3K27me3 at *FT* chromatin (Jeong et al., 2009; Yang et al., 2010). The relative levels of H3K4me3 and H3K27me3 play a key role in the regulation of *FT* expression because H3K4 and H3K27 trimethylation act antagonistically at the *FT* locus (He, 2012).

FT expression is induced by ambient warm temperature via the thermosensory pathway, and H2A.Z-containing nucleosomes mediate this response at the *FT* chromatin (Blázquez et al., 2003; Kumar and Wigge, 2010).

ARP6 encodes a subunit of the SWR1 chromatin remodeling complex, which is necessary for the deposition of the histone variant H2A.Z in the region around the *FT transcription start site* (*TSS*). Eviction of H2A.Z nucleosomes at higher temperatures would thereby facilitate *FT* transcription by Pol II (Kumar and Wigge, 2010). Loss of ARP6 (SWR1) function leads to a temperature- insensitive *FT* activation and early flowering independently of CO (Kumar and Wigge, 2010).

1.4. Chromatin organization and nuclear matrix

The *Arabidopsis* genome was found to contain about 25,500 genes encoding proteins and 125 million base pairs of DNA distributed among five chromosomes. In the eukaryotic nucleus, DNA, carrying the genetic information, is packaged with proteins into higher-order chromatin. The packing of DNA into chromatin is important for DNA dependent processes, including DNA recombination, replication, repair and transcription. The nucleosome, the basic packaging unit of chromatin, consists of approximately 146 base pairs of DNA wrapped around an octamer of core histone proteins containing two molecules each of H2A, H2B, H3 and H4 (Kornberg, 1974). This structure is more condensed to the chromatin fiber.

In view of the loop domain model, these fibers are attached at their bases to the nuclear matrix/scaffold, and the unanchored fiber loops out from

the point of attachment (Rudd et al., 2004). Chromatin attachment to the nuclear matrix is not random. Such chromatin loops occur at specific stretches of genomic DNA sequences known as matrix attachment regions (MARs), also called scaffold attachment region (SAR) which is a stretch of AT-rich DNA sequence (ATR) of high affinity (Rudd et al., 2004; Tetko et al.,2006). This looping is important for the structural organization of chromatin and has been involved in the functional compartmentalization of the genome (Schneider and Grosschedl, 2007).

Nuclear matrix/scaffold is a network of nonchromatin fibrous proteins and somewhat analogous to cellular cytoskeleton (Pederson, 2000). Experimentally, it have been defined an insoluble structure that remain inside the nucleus after removal of basic proteins and histones (Aravind and Landsman, 1998).

MARs are found at the boundaries of transcription, often found near *cis*-acting regulatory sequence and core origin replication (ORIs) (Wang et al., 2010). Therefore, its function involved with several biological processes such as DNA replication, transcription, repair, splicing and recombination (Wang et al., 2010).

However, not all potential MARs are bound to the nuclear matrix at all times. MARs are dynamically bound to the nuclear matrix in cell type- and/or cell cycle-specific manners by MAR-binding proteins (Purbey, 2009).

Currently various MAR-binding factors have been identified in yeast, animals, and plants (Tetko et al., 2006; Wang et al., 2010).

in silico analysis, 21,705 putative MARs predicted in the same order of magnitude as 26,027 *Arabidopsis* genes using the SMARTest software (Rudd et al., 2004). These regions are approximately from 300bp to several kilobases in length and are present in all higher eukaryotes, including mammals and plants (Bode et al., 1996: Allen et al., 2000). A genome-scale study of gene expression patterns in conjunction with screening of potential intragenic MARs has shown that *Arabidopsis* genes possessing intragenic MARs tend to have low transcription levels irrespective of plant tissues and organs and differentially regulated throughout the plant growth stages (Rudd et al., 2004; Tetko et al., 2006).

Therefore, MARs act as a structural determinant of chromatin organization and recruit multiple MAR-binding factors that facilitate remodeling of the chromatin structure in regulating gene expression (Wang et al., 2010).

1.5. Functions of AT-hook DNA binding proteins

The AT-hook is a small DNA binding protein motif which has a core consensus sequence of Pro-Arg-Gly-Arg-Pro, with R-G-R-P as variant, flanked on either side by a number of positively charged lysine/arginine

residues (Reeves and Nissen, 1990; Reeves, 2001). The AT-hook motifs binds to the minor grooves of AT-rich DNA in matrix attachment regions (MARs) of target DNA sequences (Reeves, 2001) Therefore AT-hook containing proteins may contribute to a functional nuclear architecture by binding to the nuclear matrix, and may also be structural components and that remain inside the nucleus after removal of basic proteins and histones (Aravind and Landsman, 1998). AT-hook motif appears an auxiliary protein motif cooperating with other DNA-binding activities and facilitating changes in the structure of DNA either as a polypeptide on its own (e.g. HIGH MOBILITY GROUP A (HMGA) or as part of a multidomain protein. (Aravind and Landsman, 1998)

The AT-hook motif is highly conserved in evolution from bacteria to humans and found in single or multi copies in a large number of other, non-HMGA proteins, many of which are transcription factors or components of chromatin remodeling complexes (Aravind and Landsman, 1998). Various AT-hook containing proteins are involved in many nuclear processes including transcriptional regulation, chromatin structure and cell division processes (Reeves, 2001; Reeves, 2010). In mammals, diverse AT-hook proteins have been identified in diverse protein groups, including HMGA proteins and SPECIAL AT-RICH SEQUENCE BINDING PROTEINS (SATB1).

HMGA protein is non-histone chromosomal protein and contains either 3 or 4 AT-hook domains. HMGA proteins act architectural transcription factors to influence a wide variety of normal biological processes including cell growth, proliferation, differentiation and death. They regulate gene expression through AT-hook region by changing the DNA conformation upon binding to differently spaced AT-rich regions in the DNA and/or direct interaction with other several transcription factors (Reeves, 2010).

Characterized function of AT-hook protein SATB1 is another quite well-studied as MAR binding protein, SATB1 acts predominantly as a repressor of numerous genes in tissue- or cell type-specific regulation (Cai et al., 2003; Han et al., 2008). The binding of SATB1 regulates gene expressions in the target chromatin by inducing structural changes of chromatin (Cai et al.,2003; Han et al.,2008) and recruitment of chromatin modifiers including HDAC1 (Yasui et al., 2002: Kumar et al., 2005). These chromatin modifiers have been suggested to suppress local or long distance gene expression via histone deacetylation and nucleosome remodeling through MARs associated with SATB1 (Yasui et al., 2002: Kumar et al., 2005). Although SATB1 has been usually demonstrated to transcriptional repressor, it can also act as a transcriptional activator according to the physiological context and post-translational modification status of SATB1 (Purbey et al., 2009).

In plants, a series of AT-hook proteins plays a role in developmental processes, such as flowering transition, and stress responses (Weigel et al., 2000; Matsushita et al., 2007; Lim et al., 2007; Street et al., 2008; Vom Endt et al., 2007; Xiao et al., 2009; Ng et al., 2009; Lu et al, 2010). Several AT-hook motif nuclear localized (AHL) proteins have been functionally studied in diverse aspects of plant growth, developmental processes and stress responses in *Arabidopsis*.

AT-HOOK PROTEIN OF GA FEEDBACK REGULATION1 (AGF1) /AHL25 is a critical for maintaining the negative feedback regulation of *GA3 oxidase* gene in gibberellin signalling (Matsushita et al., 2007). SUPPRESSOR OF PHYTOCHROME B-4 #3(SOB3)/AHL29 and ESCAROLA (ESC)/ORESARA7 (ORE7)/AHL27 repress hypocotyl elongations in light-grown seedlings (Street et al., 2008). ESC/ORE7/AHL27 also acts as a negative regulator of leaf senescence (Lim et al., 2007). *Catharanthus roseus* AHLs have been shown to regulate the level of AP2 transcription factors in response to jasmonic acid (Vom Endt et al., 2007). In addition, GIANT KILLER (GIK)/AHL21 controls in organ patterning and differentiation in flower development and plant meristem regulation (Ng et al., 2009). Furthermore, AHL22 is involved in the regulation of flowering and hypocotyl growth (Xiao et al., 2009). Meanwhile, overexpression of *AHL20* gene suppresses plant innate immune responses (Lu et al, 2010). Similarly,

transient expressions of AHL15, AHL19, and AHL27 in protoplasts have also been implicated in defence responses (Lu et al, 2010).

It has been known that MARs link AHL proteins with chromatin modifications. In *Arabidopsis*, ESC/ORE7/AHL27 controls chromatin architecture by modification of the distribution of H2B (Lim et al., 2007). In addition, AHL21/GIANT KILLER (GIK) binds to putative MARs in the *ARF* promoter and represses *AUXIN RESPONSE FACTOR 3* (*ARF3*) expression associated with repressive dimethylation H3K9 during floral development (Ng et al., 2009).

1.6. The Purpose of this research

In this study, I have figured out that MAR binding protein AHL22 provides a novel mechanism to control the floral integrator *FT* expression. I have shown that *FT* is negatively regulated by AHL22, and that the AHL22-mediated *FT* regulation is involved in epigenetic changes of the chromatin.

In *Arabidopsis*, FT has a central role in flowering time regulation, because several flowering pathways, including long day, vernalizaion, autonomous pathways and temperature-dependent pathways, are integrated into the *FT* expression. As mentioned above, the regulatory mechanism of *FT* is quite complicated. Although epigenetic regulation of the floral activator *FT*

is one of the critical factors that determine flowering, chromatin modifications via FT are largely unknown.

In particular, because AHL22 is expressed in various regions of plant tissues in this study, I characterized the spatial and temporal expression patterns of *AHL22* and *FT* to understand their regulation. I found that AHL22 regulate *FT* expression in the vascular tissues of leaves, which suggests that AHL22 and FT may have leaf-specific functions.

In addition, my study has also provided new perception for the understanding of flowering repression in *Arabidopsis*. I have shown that AHL22 effectively represses *FT* expression. This repression is related to chromatin modifications by H3 acetylation and H3K9me2. AHL22 directly binds to an ATR sequence element within the *FT* locus by recruiting a subset of histone deacetylases and/or methyltransferases. I propose that the MAR binding protein AHL22 acts as a chromatin remodeling factor that represses *FT* expression during floral transition in *Arabidopsis*.

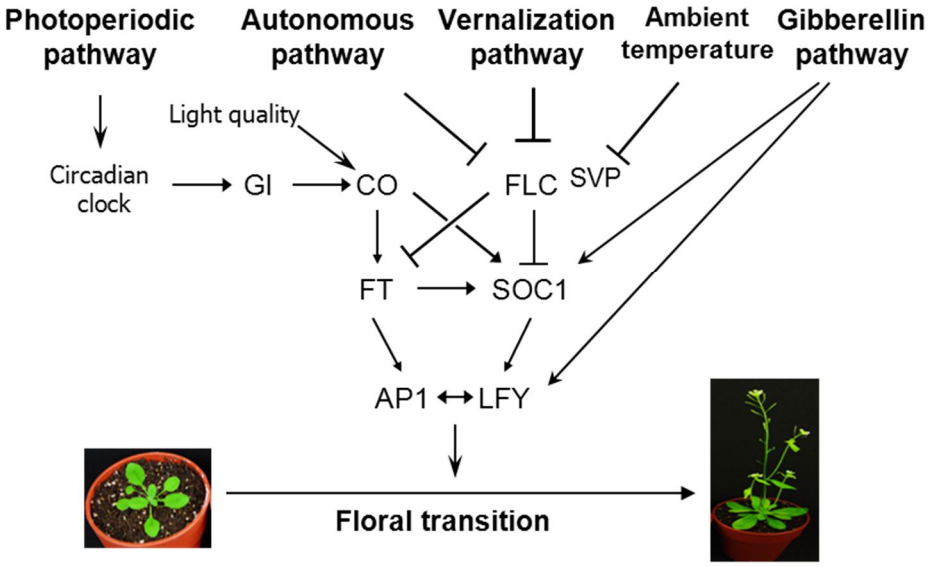

Figure 1. Genetic pathways controlling flowering time in *Arabidopsis*.

Genetic pathways monitor the seasonal changes in day length and cold temperature, as well as other local environmental and endogenous signals. The signals from these pathways are integrated to flowering time integrators; *FT*, *SOC1* and *LFY*. Expression of the floral promoters leads to upregulation of *LFY* and *AP1*, triggering flowering. The floral repressor, *FLC*, is the major target of the autonomous and vernalization pathways. And the *CO* has the function of integrating circadian clock and light signals in photoperiodic pathways. Lines with arrows indicate upregulation of gene expression; lines with T-bar indicate gene repression.

II. INTRODUCTION

The timing of flowering initiation is regulated through coordinated interactions of developmental programs, such as gibberellic acid (GA), and seasonal cues, including photoperiod, exposure to prolonged low temperature (vernalization), and ambient temperature (Amasino, 2010; Simpson and Dean, 2002; Blázquez et al., 2003). The developmental and environmental signals converge to regulate floral integrators, such as *FT*, *SUPPRESSOR OF OVEREXPRESSION OF CONSTANS 1* (*SOC1*), and *LEAFY* (*LFY*) (Simpson and Dean, 2002). The *FT* and *SOC1* integrators are also regulated by the floral repressor *FLOWERING LOCUS C* (*FLC*) that incorporates vernalization and autonomous signals into the flowering genetic network (Amasino, 2010; Simpson and Dean, 2002).

Expression of flowering time genes is modulated through various molecular and biochemical mechanisms in addition to the ordinary gene transcriptional regulation. Examples include controlled RNA metabolism, which is governed primarily by RNA-binding proteins and microRNAs (miRNAs), and epigenetic regulation, which is mediated mainly by histone modifications and DNA methylation (Simpson, 2004; Jones-Rhoades et al., 2006; He, 2009; Yaish et al., 2011).

Several RNA-binding proteins have been shown to regulate RNA processing and selection of polyadenylation sites in their own genes and *FLC* gene (Simpson, 2004; Liu et al., 2010). miRNAs regulate posttranscriptionally flowering time genes. miR156 suppresses a subset of genes encoding SQUAMOSA PROMOTER BINDING PROTEIN LIKE (SPL) transcription factors that promote flowering (Jones-Rhoades et al., 2006). miR172 induces degradation of gene transcripts encoding a small group of APETALA2 (AP2)-like transcription factors that act as floral repressors (Jones-Rhoades et al., 2006).

Expression of flowering time genes is also regulated by epigenetic mechanisms that include posttranslational modifications of histone and nonhistone proteins. Regulation of flowering initiation by histone modifications has been studied extensively in *FLC* chromatin. Molecular characterization of *FLC* repressors and activators in recent years has shown that at least three regulatory systems, vernalization, FRIGIDA (FRI), and autonomous pathway components, regulate FLC activity by modifying the *FLC* chromatin. It is known that specific lysine (K) residues in the N-terminal region of H3 are either methylated or acetylated (He, 2009). H3 trimethylation at Lys-4 and acetylation are associated with active *FLC* expression. In contrast, H3 deacetylation and methylation at Lys-9 and Lys-27 repress the *FLC* expression (He, 2009).

Nuclear matrix is a network of filamentous proteins and somewhat analogous to cellular cytoskeleton (Pederson, 2000). Organization of the nuclear matrix is regulated in a temporal and spatial manner during the cell cycle (Rudd et al., 2004; Tetko et al., 2006). It also contributes to dynamic chromatin reorganization occurring during DNA metabolism and gene expression (Pederson, 2000; Rudd et al., 2004; Tetko et al., 2006). Matrix attachment region (MAR), which is also called scaffold attachment region (SAR), is a stretch of AT-rich DNA sequence (ATR) that guides binding of genomic DNA to the nuclear matrix (Rudd et al., 2004; Tetko et al.,2006). Therefore, MAR acts as a structural determinant of chromatin organization and recruits multiple MAR-binding factors that facilitate remodeling of the chromatin structure in regulating gene expression (Wang et al., 2010).

Various MAR-binding factors have been identified in yeast, animals, and plants (Tetko et al., 2006; Wang et al., 2010). A major group of the MAR-binding factors possesses a protein motif, called AT-hook that consists of 9-12 residues (Aravind and Landsman, 1998). In animals, many AT-hook proteins have been identified in diverse protein groups, and their roles have been demonstrated in different aspects of gene regulation (Aravind and Landsman, 1998; Reeves, 2010).

In plants, a series of AT-hook proteins plays a role in developmental processes, such as flowering transition, and stress responses (Weigel et al., 2000; Matsushita et al., 2007; Lim et al., 2007; Street et al., 2008; Xiao et al., 2009; Ng et al., 2009; Lu et al, 2010). One example is the AT-hook motif nuclear localized 22 (AHL22) protein that belongs to the AHL family consisting of 29 members in *Arabidopsis* (Fujimoto et al., 2004). Overexpression of the *AHL22* gene delays flowering, and *FT* expression is reduced in the transgenic plants (Xiao et al., 2009). In contrast, silencing of four *AHL* genes (*AHL22*, *AHL18*, *AHL27*, and *AHL29*) promotes flowering, suggesting that the *AHL22* gene, and some other *AHL* genes as well, acts as a floral repressor, possibly by modulating *FT* expression.

Here, I show that the AHL22 protein binds to an ATR sequence element within the *FT* locus, which has previously been predicted as a intragenic MAR (Rudd et al., 2004), and regulates *FT* expression by recruiting a subset of histone deacetylases, such as HDA1/HDA19, HDA6, and HDA9. H3 acetylation was significantly reduced in the *AHL22*-overexpressing OE-*AHL22* mutant. I also found that H3 K9 dimethylation in the *FT* chromatin was elevated in the mutant, suggesting that AHL22 may also interact with histone methyltransferases. These observations indicate that the *FT* chromatin is coordinately regulated through H3 acetylation and methylation during floral transition.

III. MATERIALS AND METHODS

3. 1. Plant materials and growth conditions

Arabidopsis thaliana lines used were in Columbia (Col-0) background. *Arabidopsis* plants were grown in a controlled culture room at 23℃ under long days (LDs, 16-h light/8-h dark). To produce transgenic plants overexpressing *Arabidopsis* genes, the gene sequences were subcloned into the binary pB2GW7 vector under the control of the Cauliflower Mosaic Virus (CaMV) 35S-promoter (Invitrogen). The loss-of-function mutants *ahl22-1* and *ahl22-2* (SALK-018866 and SALK-143279, respectively) were isolated from a pool of T-DNA insertion lines deposited in the *Arabidopsis* Biological Resource Center (ABRC, Ohio State University).

3. 2. Isolation of OE-*AHL22* mutant

The OE-*AHL22* mutant was isolated from an *Arabidopsis* mutant pool that has been produced by randomly integrating the activation tagging vector pSKI015 that contains the CaMV 35S enhancer element into the genome of Col-0 plants (Kim et al., 2006). The presence of single T-DNA insertion event in the OE-*AHL22* mutant was verified by genomic Southern blot analysis using the 35S enhancer sequence as probe. The flanking genomic sequences of the T-

DNA insertion site were determined by a plasmid rescue method (Weigel et al., 2000).

3. 3. Analysis of transcript levels

Transcript levels were examined by either Southern blot hybridization of semi-quantitative RT-PCR products or by quantitative real-time RT-PCR (qRT-PCR). RNA sample preparations, PCR conditions, and data processing have been described previously (Kim et al., 2006).

qRT-PCR was carried out in 96-well blocks with the Applied Biosystems 7500 Real-Time PCR System using the SYBR Green I master mix in a volume of 20μl. The two-step thermal cycling profile used was denaturation for 15 sec at 94 °C and extension for 1 min at 68 °C. The comparative $\Delta\Delta C_T$ method was used to evaluate the relative quantities of each amplified product in the samples. The threshold cycle (C_T) was automatically determined for each reaction by the system set with default parameters. The specificity of amplifications was determined by melt curve analysis of the amplified products using the standard method installed in the system. The *eIF4A* (*eukaryotic initiation factor 4A*) gene (At3g13920) was included in the reactions as internal control for normalizing the variations in the cDNA amounts used. The RT-PCR and qRT-PCR primers used are listed in Table 1 and 2.

3. 4. Flowering time measurements

Plants were grown in soil under LDs until flowering. Flowering times were determined by counting the number of rosette leaves at bolting. Fifteen to twenty plants were counted and averaged for each measurement.

3. 5. AHL22 binding to *FT* DNA

Binding of AHL22 to *FT* DNA was examined using recombinant maltose binding protein (MBP)-AHL22 fusion protein essentially as described previously (Parviz et al., 1998) but with some modifications. The recombinant MBP-AHL22 fusion protein was produced in Escherichia coli strain BL21-codonPlus (DE3)-RIL (Stratagene, La Jolla, CA). After induction for 5 h at room temperature, E. coli cells were harvested and resuspended in lysis buffer A (20 mM Tris-HCl, pH 7.4, 200 mM NaCl, 1 mM EDTA, and 10 mM β-mercaptoethanol) containing protease inhibitor cocktail (Sigma) and 1 mM PMSF. The cells were lysed by French press (8500 psi, three times). The cell lysates were sonicated for 30 sec twice and centrifuged at 20,000 X g for 20 min. The supernatants were stored at -80℃ until use.

For purification of the fusion protein, 1 ml of cell lysates was mixed with amylose resin (NEB) and incubated at 4 °C for 2 h. The resin was washed 3 times with fresh lysis buffer A.

Bound proteins were eluted with 1 X SDS-PAGE loading buffer, separated on 10% SDS-PAGE, and transferred to polyvinylidene fluoride (PVDF) membrane. The air-dried membrane blot was immersed in binding buffer (25 mM HEPES, pH 8.00, 60 mM KCl, 1 mM EDTA, 1 mM DTT, and 6 M guanidine hydrochloride) and gently shaken for 10 min at 4 °C. Renaturation of the bound proteins and MAR binding assays were carried out as described previously (Parviz et al., 1998).

3. 6. Nuclei isolation for protein analysis

Nuclei was isolated as described (Ng et al., 2009) with some modifications. The isolated nuclei were washed once with RSB buffer (10 mM NaCl, 3 mM $MgCl_2$, 10 mM Tris-HCl, 0.5 mM PMSF, pH 7.4) and a fraction was kept as a total nuclear control. The remaining sample was digested with 50 U of DNaseI (Roche) in RSB containing 0.3 M sucrose and 1 mM $CaCl_2$ for 2 h at room temperature. After centrifugation, pellets were resuspended in RSB and an equal volume of high-salt buffer I (4 M NaCl, 20 mM EDTA, 20 mM Tris-HCl, pH 7.4) and incubated for 30 min at 4℃. After centrifugation, the pellets were further extracted twice with high salt buffer II (2 M NaCl, 20 mM EDTA, 20 mM Tris-HCl, pH 7.4, 0.25 mg/mL BSA). After high-salt extractions, the matrices were washed with RSB buffer containing 0.25 M sucrose and 0.25 mg/mL BSA and resuspended in the same buffer. Total

nuclear lysates and the resuspended matrices were used for western analysis. Anti-MYC were used to detect AHL22 and CO proteins.

3. 7. Chromatin immunoprecipitation assays (ChIP)

ChIP assays were performed as described previously (Yang et al., 2011) using 2-week-old plants grown under LDs on ½ X Murashige & Skoog (MS)-agar plates (hereafter, referred to as MS-agar plates). Briefly, rosette leaves were vacuum-infiltrated with 1% formaldehyde for cross-linking and ground in liquid nitrogen after quenching the cross-linking process. Chromatin preparations were sonicated into 0.5~1-kb fragments. Specific antibodies against MYC (Catalog Number 05-419), H3ac (Catalog Number 06-599), H3K9me2 (Catalog Number 07-212), and H3K27me3 (Catalog Number 07-449) (Millipore, Billerica, MA) were added to the chromatin solution, which was precleared with salmon sperm DNA/ Protein A agarose beads. The precipitates were eluted from the beads. Cross-links were reversed, and residual proteins were removed by incubation with proteinase K. DNA was recovered using the QIAquick spin column (Qiagen, Valencia, CA). Quantitative PCR was used to determine the amounts of genomic DNA enriched in the chromatin samples. The primers were designed to amplify DNA fragments of 100~200 bp (Table 2).

3. 8. Electrophoretic mobility shift assays (EMSA)

EMSA assays were carried out as described previously (Yang et al., 2011) using recombinant MBP-AHL22 fusion protein. Double-stranded DNA fragments were end-labelled with [γ-^{32}P]-ATP using T4 polynucleotide kinase. The radiolabelled DNA fragments were incubated for 30 min at room temperature with 1 μg of the MBP-AHL22 fusion protein in binding buffer (10 mM Tris-HCl, pH 7.6, 50 mM NaCl, 1 mM EDTA, 5 mM DTT, 5% glycerol) supplemented with 100 ng of poly(dI-dC) in the presence or absence of competitor DNA fragments. The reaction mixtures were resolved on 4% non-denaturing polyacrylamide gel. The gel was dried on Whatman 3 MM paper and exposed to X-ray films.

3. 9. Subcellular localization assays

A full-size AHL22 cDNA was fused in-frame to the 3' end of a green fluorescence protein (GFP)-coding sequence in the p2FGW7 vector (Invitrogen), and the fusion construct was transformed into Col-0 plants. Lateral roots were subject to fluorescence microscopy.

For bimolecular fluorescence complementation (BiFC) assays, a full-size AHL22 cDNA was fused in-frame to either the 5' end of a DNA sequence encoding the N-terminal half of EYFP in the pSATN-nEYFP-C1 vector (E3081) or to the 3' end of a DNA sequence encoding the C-terminal half of

EYFP in the pSATN-cEYFP-C1 vector (E3082). The pSAT vectors were kindly provided by Stanton Gelvin (Purdue University). The expression constructs were cotransformed into *Arabidopsis* protoplasts by a polyethylene glycol-calcium transfection method (Yoo et al., 2007). YFP signals were analyzed 14-18 h after transfection by fluorescence microscopy using the Zeiss LSM510 confocal microscope (Carl Zeiss, Yena, Germany).

3. 10. *in vitro* pull-down assays

HDAC cDNAs were amplified by RT-PCR and subcloned into the pGBKT7 vector, which contains the SP6 RNA polymerase promoter upstream of multiple cloning sequences. [35S]-labelled HDAC proteins were prepared by in vitro transcription/translation using the TNT SP6 wheat germ extract-coupled system (Promega, Madison, WI). The MBP-mAHL22 gene fusion was subcloned into the pMAL-c2X E. coli expression vector, and recombinant MBP-mAHL22 protein was prepared as described with the recombinant MBP-AHL22 protein above. *in vitro* pull-down assays were carried out as described previously (Hong et al., 2011) using 5 μl of ^{35}S-labelled HDAC polypeptides and 5 μg of MBP alone or MBP fusion proteins.

3. 11. Histochemical staining

A promoter region consisting of approximately ~2-kbp sequence upstream of the transcription start site of *AHL22* gene was transcriptionally fused to a *β*-Glucuronidase (GUS)-coding sequence, and the p*AHL22-GUS* fusion was transformed into Col-0 plants. The p*FT-GUS* construct has been described previously (Takada et al., 2003). Plant sample processing and histochemical detection of GUS activities were carried out as described previously (Yang et al., 2011).

3. 12. Phylogenetic analysis

Amino acid sequences of AT-hook proteins in *Arabidopsis* were obtained from TAIR. Phylogenetic trees were based on multiple alignments done with CLUSTAL W and performed with PHYLIP (Department of Genetics, University of Washington, Seattle, WA).

Primers	Sequences
TUB-F	5′-TCACCTTCTTCATCGCAGTT
TUB-R	5′-ATTTGCACCGTACTTTGACT
eIF4a-F	5′-TACTGGGAAAACAGCAACTT
eIF4a-R	5′-TGATCTCAAGAGCTTCTGGT
CO-F	5′-ATCAGCGAGTTCCAATTCTA
CO-R	5′-GGAACCATTGTCGTTGTAGT
SOC1-F	5′-CTGAGGCATACTAAGGTCG
SOC1-R	5′-GAACAAGGTAACCCAATGAA
FT-F	5′-AGACGTTCTTGATCCGTTTA
FT-R	5′-GTAGATCTCAGCAAACTCGC
FCA-F	5′-GTTTCATCTTCTGCCACATT
FCA-R	5′-TAAATTTTGGTTTGGTTGCT
FVE-F	5′-GTTGTTTGATCGTAGGAAGC
FVE-R	5′-AACATGCGACTTGAACTTCT
FLC-F	5′-AGCGAATTGAGAACAAAAG
FLC-R	5′-GCTCCCACATGATGATTATT
SPY-F	5′-AACTACCGCTGAATAAACCA
SPY-R	5′-GGTGAACTCTGTTTTTGAGC
RGA-F	5′-TCCATTACTCTCCTCCACAC
RGA-R	5′-CAAGAAGGGTTATCTGAGGAA
LFY-F	5′-TTGAAGCTTCTTCGTCTAGG
LFY-R	5′-ATGAGCCCTAAAGAGCTTCAGAATCTG
AP1-F	5′-GCGGCGAAGCAGCCAAGGTTGCAGTTG
AP1-R	5′-CTAAGAACAAACCAAAACCG
AHL22-F	5′-CTAAGAACAAACCAAAACCG
AHL22-R	5′-GCAACCTTGTATAACGAC
At2g45420-F	5′-CTCAAGAGGTTCTCATCAGCAGTA
At2g45420-R	5′-CTTGGAGGTCATGACTGTTT

Table 1. Primers used in RT-PCR.

F, forward primer; R, reverse primer.

Primers	Sequences
eIF4a-real-F	5′-TGACCACACAGTCTCTGCAA
eIF4a-real-R	5′-ACCAGGGAGACTTGTTGGAC
FT-M1-F	5′-GACATGTAGCTACTACCTTTTTTCTATTCA
FT-M1-R	5′-CAATGGAGATATTCTCGGAGGTG
FT-M2-F	5′-GTTTGTGCACTAACTCAACTCTTTAATTA
FT-M2-R	5′-ATTTTATATGTCTCCTTCTATTAAATGTAAAATG
FT-M3-F	5′-CAACTTCGAGAGTGCGATGC
FT-M3-R	5′-GACCACTTTAAAGTGAAAAAAACAAAT
FT-P1-F	5′-CCGAGTTAATGCAAATCCGA
FT-P1-R	5′-GAACGTCTCCAACAACTCTGCT
AHL22-real-F	5′-TCCCAACGAGCACTCTTCAG
AHL22-real-R	5′-GTGATTATCTCCTCCTCCTCCG
FT-real-F	5′-AGACGTTCTTGATCCGTTTA
FT-real-R	5′-GGTTGCTAGGACTTGGAACATC
AP1-A-F	5′-TGATGAAACAATAATACCGTAAGCA
AP1-A-R	5′-TGGTGTTTTCCACGTGTCTTC
AP1-B-F	5′-CCATTTTTGGATTTTTTGATTAGC
AP1-B-R	5′-GATTAAACATACACCCTTCTATATGCTC
LFY-C-F	5′-CAGTCTCTCAGAACTTCGATTTGAC
LFY-C-R	5′-GAACTAAAAATACAAATTAAAGTGTGGG
LFY-D-F	5′-GATTATGGATCCTGAAGGTTTCACG
LFY-D-R	5′-AAGCAGCCGTCTGCGGTGT

Table 2. Primers used in qRT-PCR and ChIP assays.

F, forward primer; R, reverse primer.

IV. RESULTS

4. 1. Pleiotropic phenotypes of OE-*AHL22* mutant

The *AHL22*-overexpressing OE-*AHL22* mutant exhibited delayed flowering with small, curled rosette leaves (Figure 2A and 2B). It was also featured by having short siliques and altered floral structure (Figure 2C and 2D). I mapped the site of T-DNA insertion by a plasmid rescue method (Weigel et al., 2000). It was found that the T-DNA element was inserted adjacent to the *At2g45430* locus in the mutant (Figure 3A). Genomic Southern blot hybridization confirmed that there was a single T-DNA insertion event in the mutant (Figure 3B). Gene expression assays showed that the *At2g45430* gene was activated significantly in the mutant (Figure 3C), suggesting that activation of the *At2g45430* gene correlates with the OE-*AHL22* phenotypes. To examine the correlationship, the At2g45430 gene was overexpressed driven by the CaMV 35S promoter in Col-0 plants. The resulting 35S:*AHL22* transgenic plants recapitulated the OE-A*HL22* phenotypes (Figure 2A), indicating that the *At2g45430* activation underlies the OE-*AHL22* phenotypes. The At2g45430 gene has previously been named *AT-hook motif nuclear localized 22* (*AHL22*) (Xiao et al., 2009; Fujimoto et al., 2004).

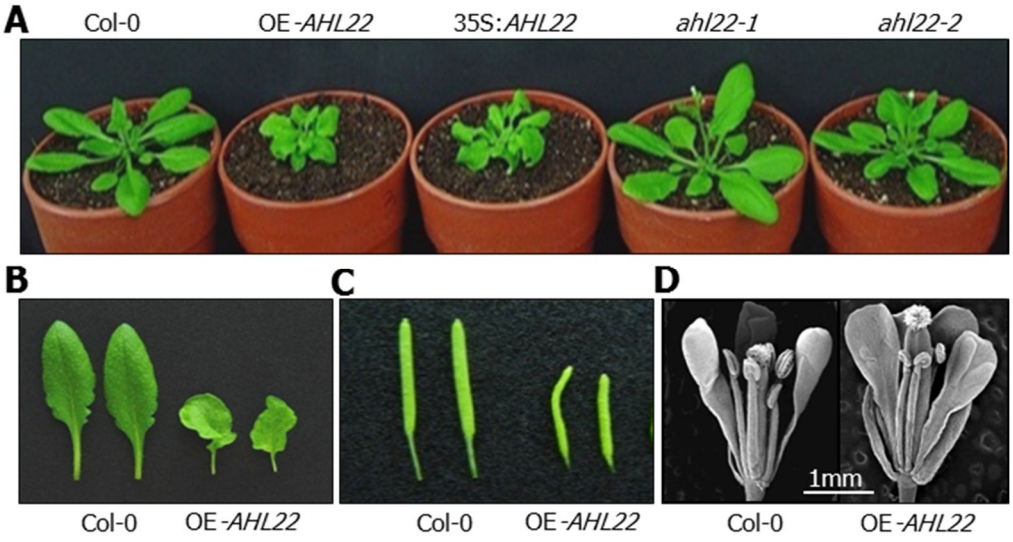

Figure 2. Phenotypic characterizations of OE-*AHL22* and *ahl22* mutants.

(A) Phenotypic comparison. Plants were grown in soil for 4 weeks under LDs before taking photographs. *AHL22* gene was overexpressed driven by the CaMV 35S promoter in Col-0 plants, resulting in 35S:*AHL22* transgenic plants.

(B) Altered leaf morphology. Two representative leaves were photographed for each plant genotype.

(C) Short, curled siliques. Two representative siliques were photographed for each plant genotype.

(D) Altered floral structure. Floral structures were compared by scanning electron microscopy. Parts of sepals and petals were removed to visualize the internal structures of flowers.

Figure 3

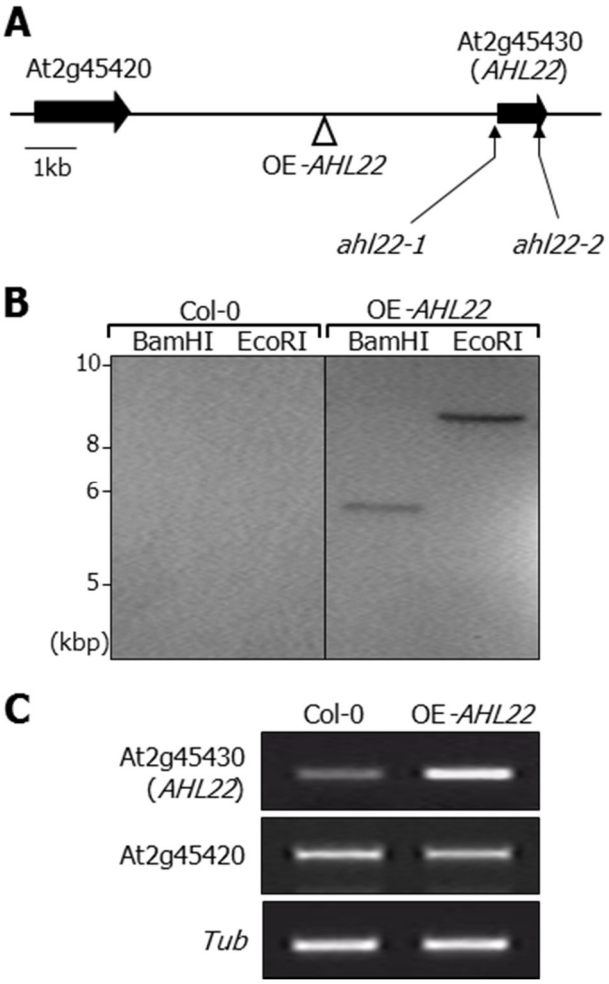
A
At2g45420
At2g45430
(AHL22)
1kb
OE-AHL22
ahl22-1
ahl22-2
B
Col-0
OE-AHL22
BamHI
EcoRI
BamHI
EcoRI
10
8
6
5
(kbp)
C
Col-0
OE-AHL22
At2g45430
(AHL22)
At2g45420
Tub

Figure 3. Molecular characterizations of OE-*AHL22* and *ahl22* mutants.

(A) Mapping of T-DNA insertion events. *AHL22* gene does not have introns. kb, kilobase.

(B) Genomic Southern blot hybridization. Genomic DNA was digested with either BamHI or EcoRI. The gel blot was probed with ^{32}P-labelled 35S enhancer sequence. kbp, kilobase pair. The result showed that there was a single T-DNA insertion event in OE-*AHL22* mutant.

(C) Activation of *AHL22* gene in OE-*AHL22* mutant. The *At2g45420* gene adjacent to the *AHL22* gene locus was included in the assays. A tubulin gene (*Tub*) was used as control for constitutive expression. Transcript levels were compared by semi-quantitative RT-PCR.

Two AHL22-deficient mutants, *ahl22-1* and *ahl22-2*, were isolated from the T-DNA insertion pool deposited in the ABRC. The knockout mutants did not show discernible phenotypes (Figure 2A), possibly because of extensive functional redundancy between AHL22 and other AHL genes (Xiao et al., 2009).

4. 2. *AHL22* encodes an AT-hook DNA-binding protein

AHL22 protein consists of 317 residues (Figure 4A and 4B). Database-assisted protein structural analysis revealed that it contains an AT hook DNA-binding motif and is identical to the previously annotated AT hook motif nuclear localized protein22 (AHL22) (Fujimoto et al., 2004). The AT hook is small sequence motif with a conserved RGRP sequence at the center and found in a subgroup of high mobility group (HMG) proteins and other DNA-binding proteins in eukaryotes. The AHL22 protein also contains the conserved PPC (plants and prokaryotes conserved) domain, which has been originally designated as domain of unknown function 296 (DUF296). In addition, AHL22 protein includes several structural motifs, including glutamine-rich, histidine-rich, and glycine-rich sequences that are frequently found in many transactivators and mediate protein-protein interactions. The hydrophobic region of the PPC is critical for nuclear localization (Fujimoto et al., 2004).

The AHL22 protein is a member of the family consisting of approximately 29 proteins (AHL1 to AHL29) having a primary structure similar to that of AHL22 (Matsushita et al., 2007). *Arabidopsis AHL* genes evolved into two phylogenetic clades. 15 paralogues showed a similar structure to AHL22 containing intronless with only single copy of AT-hook motif at the center and a PPC/DUF296 domain (Figure 4 and Figure5). Another clade including AHL1 has intron with either one or two AT-hook motifs and a PPC/DUF296 domain. None of the animal proteins contains the PPC domain (Aravind and Landsman, 1998). These distinctions suggest that molecular and biochemical activities of plant AT-hook proteins might be different from the prokaryotic PPC-containing proteins and the animal AT-hook proteins.

4. 3. *FT* is repressed in OE-*AHL22* mutant

The most prominent phenotype of the OE-*AHL22* mutant was late flowering, as has been observed in *Arabidopsis* mutant overexpressing *ESCAROLA (ESC) /ORESARA7 (ORE7)/AHL27* gene (Weigel et al., 2000; Lim et al., 2007). The early-flowering phenotype of multiple *ahl* mutants also supports the role of the *AHL22* gene and probably other *AHL* genes in flowering time control (Xiao et al., 2009).

Figure 4

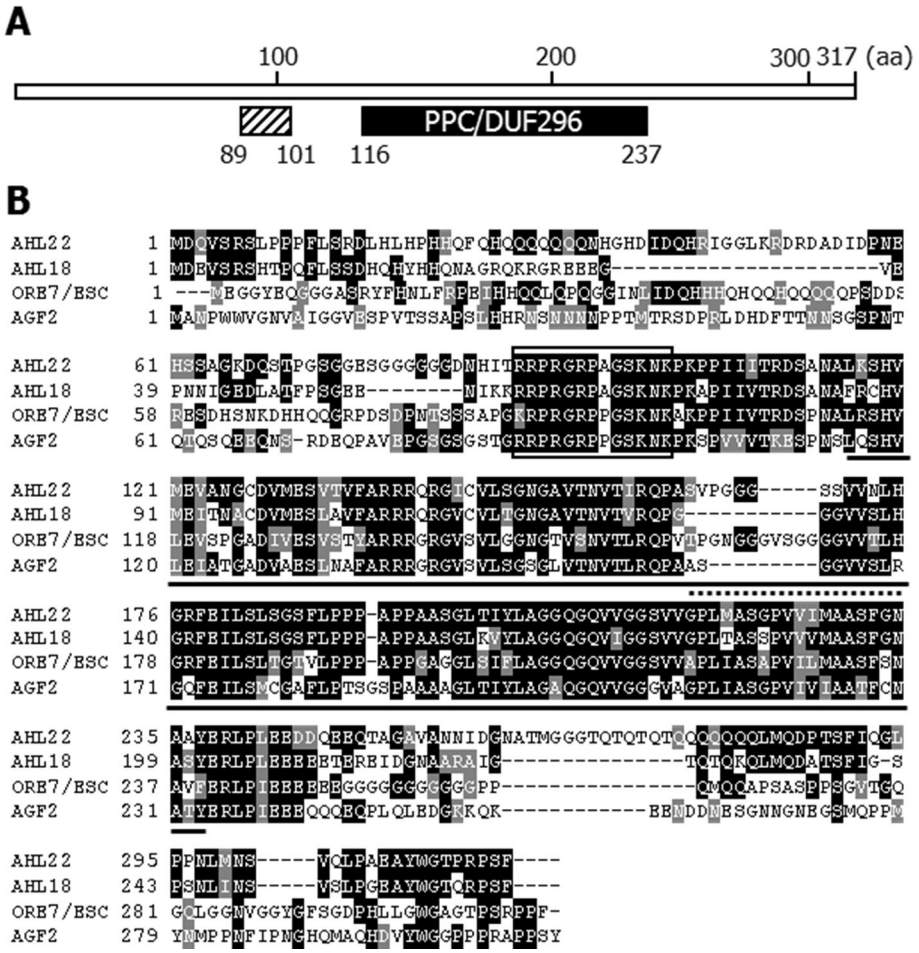
A
100
200
300 317 (aa)
PPC/DUF296
89 101 116 237
B
AHL22 1
AHL18 1
ORE7/ESC 1
AGF2 1
AHL22 61
AHL18 39
ORE7/ESC 58
AGF2 61
AHL22 121
AHL18 91
ORE7/ESC 118
AGF2 120
AHL22 176
AHL18 140
ORE7/ESC 178
AGF2 171
AHL22 235
AHL18 199
ORE7/ESC 237
AGF2 231
AHL22 295
AHL18 243
ORE7/ESC 281
AGF2 279

Figure 4. Sequence similarity of AHL22 to AHL proteins.

(A) The AHL22 protein structure. The AT hook motif (residues 89-101, hatched box) and PPC/DUF296 domain (residues 116-237, black bar) are indicated.

(B) Multiple sequence alignments of AHL22 and several AHL proteins. The sequences aligned are AHL18 (At3g60870), AHL27/ESC/ORE7 (At1g20900), and AHL15/AGF2 (At3g55560). The thin box denotes AT hook motif. The PPC domain is underlined. The hydrophobic region of the PPC domain is upperlined (dotted line).

Figure 5

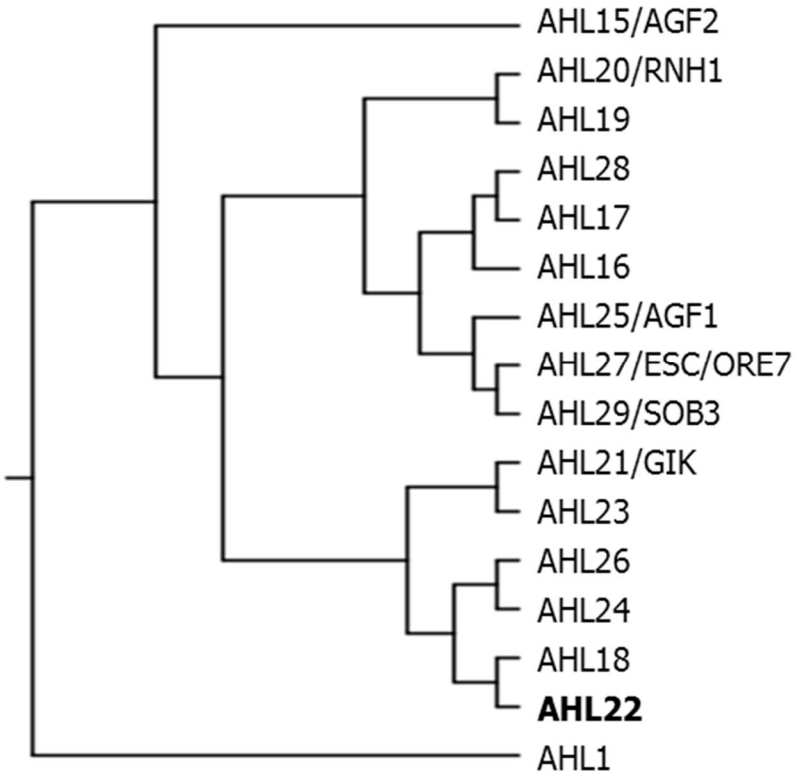
AHL15/AGF2
AHL20/RNH1
AHL19
AHL28
AHL17
AHL16
AHL25/AGF1
AHL27/ESC/ORE7
AHL29/SOB3
AHL21/GIK
AHL23
AHL26
AHL24
AHL18
AHL22
AHL1

Figure 5. Phylogenetic Analysis of *AHL* gene family in *Arabidopsis*.

Phylogenetic tree of AHL22 related proteins were compared using ClustalW and PHYLIP software. AGI and gene names: AHL1 (At4g12080), AHL15 (AGF2, At3g55560), AHL16 (At2g42940), AHL17 (At5g49700), AHL18 (At3g60870), AHL19 (At3g04570), AHL20 (RNH1, At4g14465), AHL21(GIK, At2g35270), AHL22 (At2g45430), AHL23 (At4g17800), AHL24 (At4g22810), AHL25 (AGF1, At4g35390), AHL26 (At4g12050), AHL27 (ESC/ORE7, At1g20900), AHL28 (At1g14490), AHL29 (SOB3, At1g76500) (Fujimoto et al. 2004; Matsushita et al. 2007).

Expression analysis of flowering time genes showed that *FT* gene (At1g65480) is significantly suppressed in the OE-*AHL22* mutant (Figure 6A and 6B).

LFY and *AP1* genes, which act downstream of the *FT* gene (Amasino, 2010; Blázquez et al., 2003), were also suppressed in the mutant. In contrast, expression of the *FT* gene was slightly but reproducibly elevated in the *ahl22* mutants (Figure 6A), suggesting that the late-flowering phenotype of the OE-*AHL22* mutant is at least in part caused by *FT* suppression.

To investigate the potential linkage between the late-flowering phenotype of the OE-*AHL22* mutant and *FT* gene, I compared the spatial expression patterns of the *FT* and *AHL22* genes. The p*AHL22-GUS* construct, in which a promoter region consisting of approximately 2-kb upstream of the transcription start site of the *AHL22* gene was fused transcriptionally to the GUS-coding sequence, was transformed into Col-0 plants. The p*FT-GUS* fusion has been constructed in a similar manner (Takada et al., 2003).

Histochemical assays revealed that in 8-day-old seedlings, whereas GUS activity was detected broadly in the hypocotyls, roots and vascular bundles of the leaves in the p*AHL22-GUS* transgenic plants, it was detected primarily in the vascular bundles of the leaves in the p*FT-GUS* transgenic plants (Figure 7A). Close examination of GUS distribution patterns in the leaves of 12-day-old seedlings revealed that GUS activity was detected in the vascular bundles of the basal leaf area in the p*AHL22-GUS* transgenic plants (Figure 7B).

Figure 6

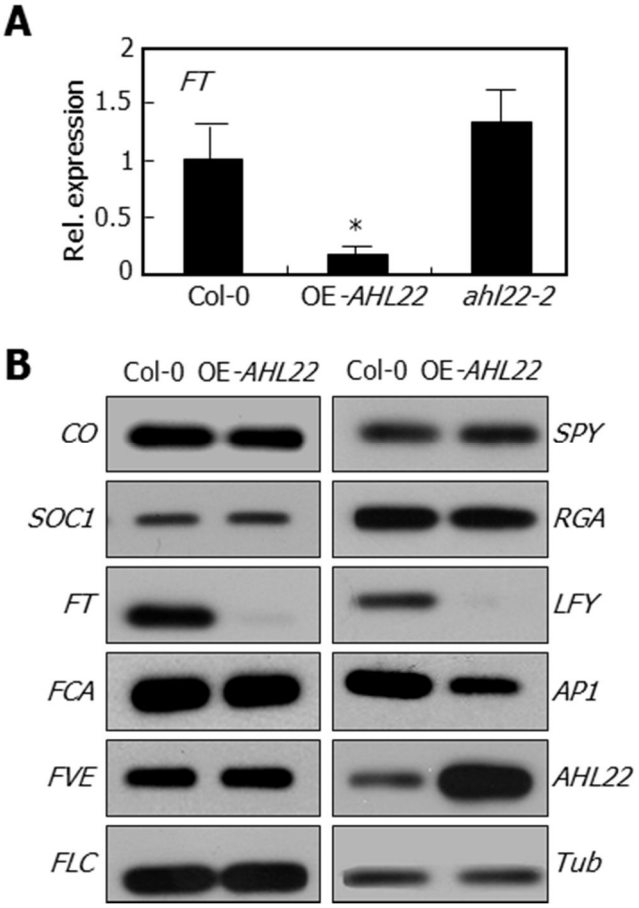
A
FT
Rel. expression
2
1.5
1
0.5
0
*
Col-0
OE-AHL22
ahl22-2
B
Col-0 OE-AHL22
Col-0 OE-AHL22
CO
SPY
SOC1
RGA
FT
LFY
FCA
AP1
FVE
AHL22
FLC
Tub

Figure 6. Expression of flowering time genes in OE-*AHL22* mutant.

(A) *FT* transcript levels. Transcript levels were determined by qRT-PCR. Biological triplicates were averaged and statistically treated using a student t-test (*P<0.01). Bars indicate standard error of the mean.

(B) Expression of flowering time genes in *OE-AHL22* mutant. Transcript levels were compared by RT-PCR-based Southern blot hybridization. A tubulin gene (*Tub*) was included as control for constitutive expression. Whole plants grown on ½ X Murashige & Skoog (MS)-agar plates (hereafter, referred to as MS-agar plates) for 2 weeks under long days (16-h light/8-h dark) were used for extraction of total RNA.

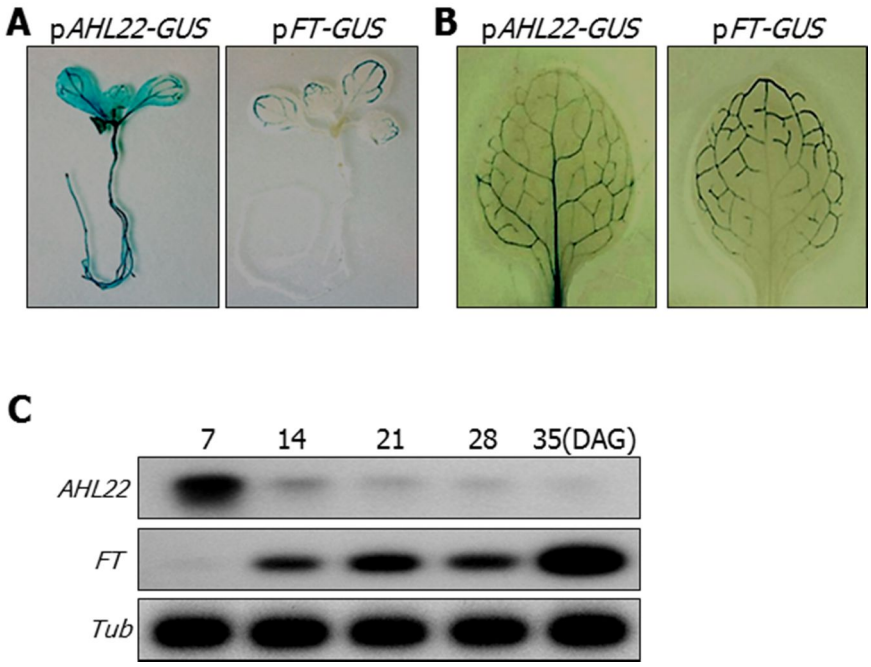

Figure 7. Spatial and temporal expression patterns of *AHL22* and *FT* genes.

(A) and (B), Expression domains of *AHL22* and *FT* genes. Whole-mount staining of 8-day-old seedlings (A) and staining of the first rosette leaves of 12-day-old seedlings (B) were displayed.

(C) Temporal expression patterns of *AHL22* and *FT* genes. Plants were grown in soil for up to 35 days after germination (DAG). Transcript levels were compared by RT-PCR-based Southern blot hybridization. A tubulin gene (Tub) was included as control for constitutive expression. Temporal expression patterns of the AHL22 and *FT* genes were compared.

In contrast, it was detected in the vascular bundles of the distal leaf area in the p*FT*-*GUS* transgenic plants, as has been observed (Takada et al., 2003).

The *AHL22* gene was highly expressed in earlier growth stages, but its expression decreased drastically during the period of 2 to 3 weeks after germination (Figure 7C), when *Arabidopsis* plants experience a transition from the juvenile to adult vegetative growth stages (Amasino, 2010). In contrast, the *FT* gene exhibited reversed expression kinetics. Together with the *FT* suppression in the OE-*AHL22* mutant, the opposite spatial and temporal expression patterns of the *AHL22* and *FT* genes further support the notion that the *FT* suppression is related with the *AHL22*-mediated late flowering.

I next examined responses of the OE-*AHL22* flowering to vernalization, exposure to a long period of low temperature (6 weeks, 4℃), GA, and photoperiod to determine genetic pathways through which AHL22 exerts its role. The OE-*AHL22* flowering was only slightly accelerated by vernalization as measured both by days to flowering and total leaf (rosette) numbers at floral initiation (Figure 8A). The late-flowering phenotype of OE-*AHL22* mutant is independent of FLC and is not strongly suppressed by vernalization.

In contrast, OE-*AHL22* mutant was significantly accelerated by exogenous GA treatment, although not complete in long days (Figure 8B).

AHL22 regulates flowering by both GA-dependent and independent mechanism in LD. Therefore, AHL22 normally respond to vernalization treatment and GA application in LD. The autonomous pathway mutants also showed late flowering and they flower later in SD than in LD through upregulation of *FLC* expression. However, FLC expression of OE-*AHL22* mutant is not affected, indicating that OE-*AHL22* mutant distinguish the autonomous pathway.

The OE-*AHL22* flowering was severely delayed under short days (SDs). The OE-*AHL22* mutant did not flower when grown under SDs (Figure 9A and B). Photoperiod pathway mutant causes late flowering in LD, but do not affect on flowering time in SD. Together, these results suggest that the AHL22-mediated flowering is not directly modulated through the known flowering pathways. Consistent with this notion, the expression of AHL22 was not alter in photoperiod mutants and those belonging to vernalization and autonomous pathways (data not shown), further supporting that AHL22 does not belong to known flowering pathways.

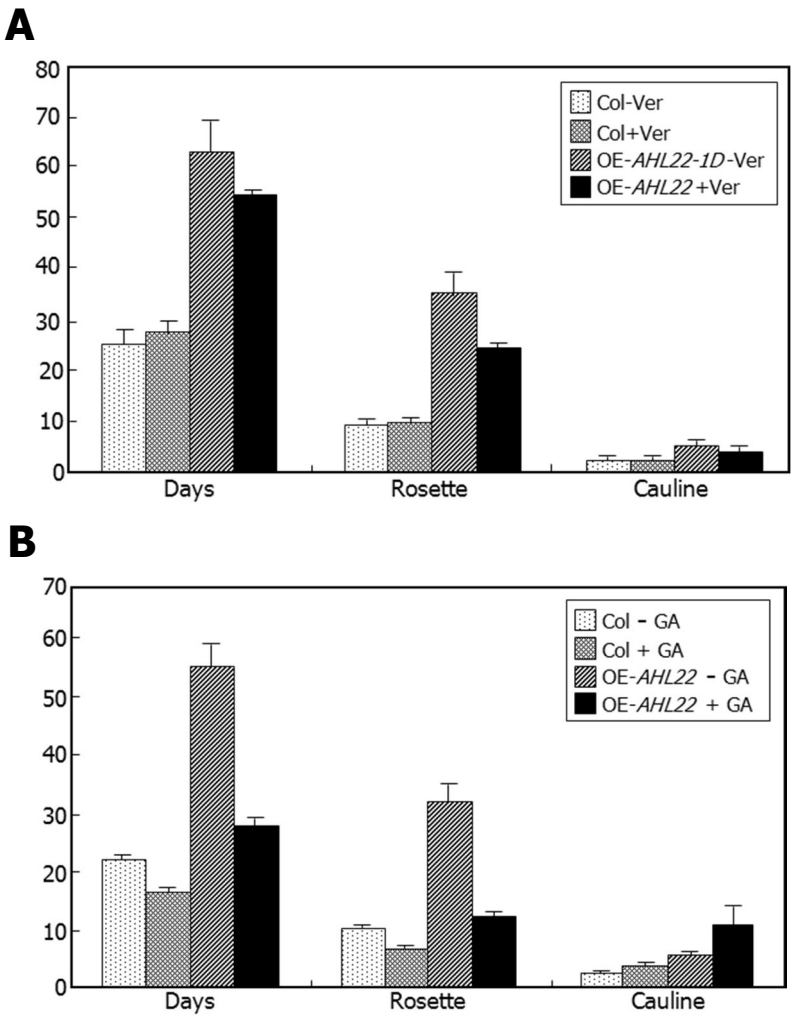

Figure 8. Flowering phenotype of OE-*AHL22* responses to vernalization and GA treatment.

(A) Response of OE-*AHL22* to vernalization treatment.

(B) Response of OE-*AHL22* to exogenous GA. Plants was sprayed with 100mM of GA twice a week until flowering.

A

Col-0 OE-*AHL22*

B

Genotypes	No. of rosette leaves
Short days	
Col-0	54.0 ± 6.4
OE-*AHL22*	ND
ahl22-1	53.3 ± 8.9
ahl22-2	54.1 ± 3.5

Figure 9. Flowering phenotype of *AHL22* mutants under SD.

(A) Flowering phenotype of OE-*AHL22* mutant under SDs. OE-*AHL22* mutant did not flower under SDs.

(B) Flowering phenotype of *ahl22* mutants under SDs (8-h light and16-h dark). (ND : Non determined)

4. 4. Binding of AHL22 to *FT* DNA

AHL proteins possess MAR-binding activity (Ng et al., 2009; Fujimoto et al., 2004). Intragenic MARs are intimately associated with gene regulation (Tetko et al., 2006). I therefore hypothesized that AHL22 might bind to intragenic MARs in the *FT* locus.

in silico mapping of the Arabidopsis genome sequence revealed that an ATR sequence element consisting of approximately ~620 nucleotides, which covers parts of introns 1 and 2 and exon 2 of the FT gene (Figure 10A), has previously been identified as a putative intragenic MAR (Rudd et al., 2004).

I first examined whether AHL22 is a bona fide nuclear matrix-bound protein using 35S:*MYC-AHL22* plants. I isolated the nuclei from the 35S:*MYC-AHL22* plants and then purified the matrix fraction by DNaseI treatment and extensive washing with high-salt buffer, which removes basic proteins and histones (Ng et al., 2009) The total nuclear protein and the matrix fraction were probed with anti-MYC that recognizes AHL22-6MYC protein. A strong AHL22 signal was observed in the matrix fraction of the nuclei. In comparison, CO (as a control) was perfectly washed away during the extraction processes, and signal was no detected in the matrix fraction on the same membrane (Figure 10B). This suggests that AHL22 binds to the nuclear matrix.

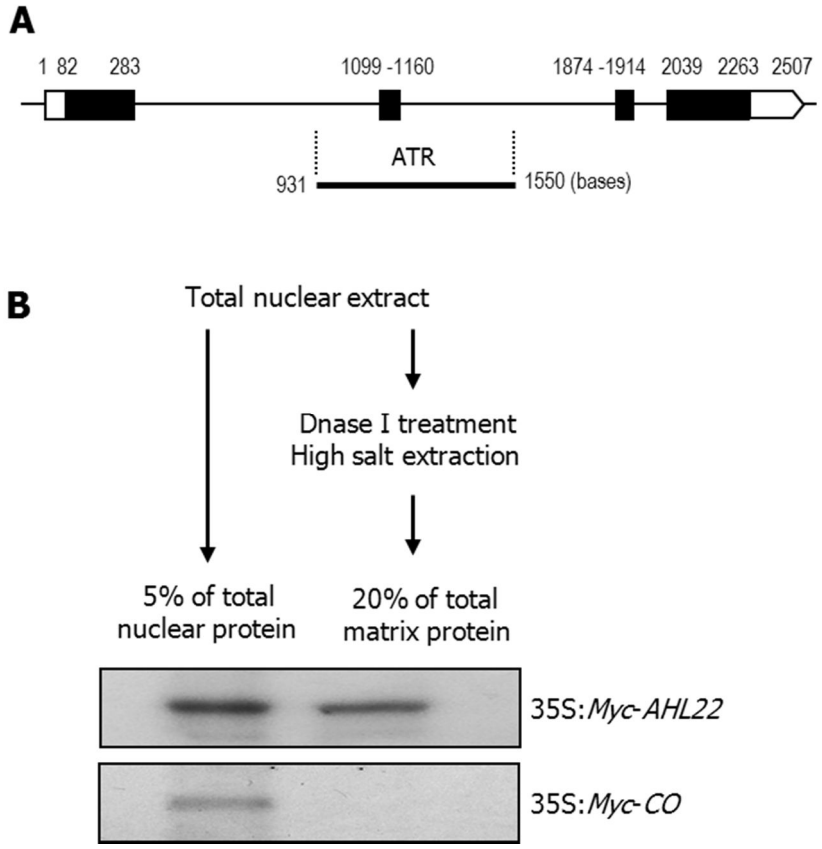

Figure 10. Binding of AHL22 to nuclear matrix.

(A) Location of ATR in *FT* locus. Black bars indicate exons, and white bars indicate untranslated regions. Putative MAR binding sequences.

(B) Binding assays on AHL22 binding to nuclear matrix.

I decided to examine whether AHL22 binds to the ATR sequence in the *FT* locus. Recombinant AHL22 protein was prepared as MBP-AHL22 fusion in *E. coli* cells. The *FT*-ATR fragment was prepared by genomic PCR and end-labelled with [γ-^{32}P]-ATP. Southwestern analysis showed that AHL22 indeed binds to the *FT*-ATR (Figure 11A).

The homeobox motif-containing ATHB2 transcription factor, which does not have the AT-hook (Schena and Davis, 1992), also bound to the *FT*-ATR. However, the ATHB2-binding DNA fragment, which is a distinct 9 bp dyad-symmetric sequence [CAAT(G/C)ATTG] (Sessa et al., 1993), specifically bound only to ATHB2, but not to AHL22, suggesting that multiple regulatory factors binds to the *FT*-ATR. Sequence comparison identified a putative AT-hook-like sequence in the ATHB2 protein (Figure 11B, upper panel). I did not examine whether the sequence motif is responsible for the binding of ATHB2 to the *FT*-ATR.

Notably, the *Arabidopsis* high mobility group A (HMGA) protein (At1g14900), which has four AT-hook motifs in the C-terminal region, did not bind to the *FT*-ATR (Figure 12), showing that not all AT-hook proteins bind to the *FT*-ATR.

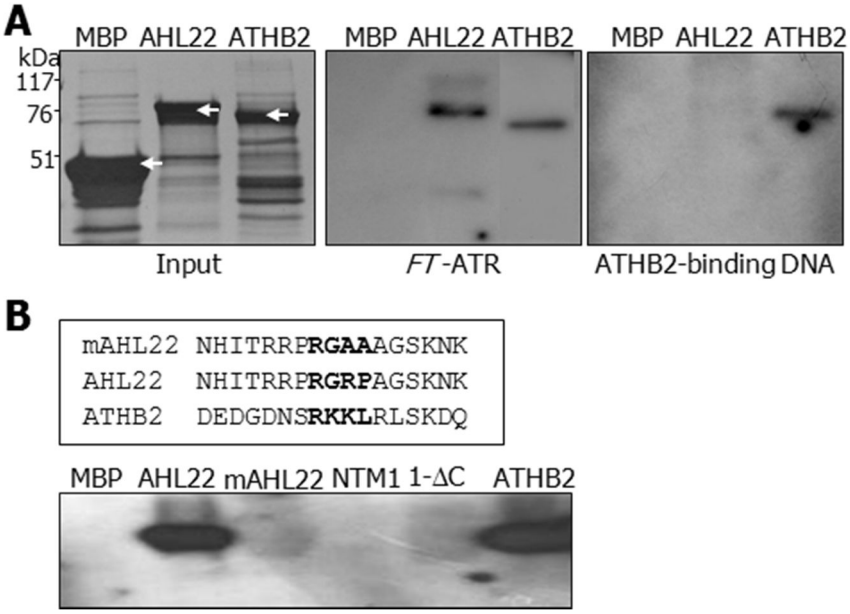

Figure 11. Binding of AHL22 to *FT*-ATR.

(A) AHL22 binding to *FT*-ATR. Recombinant AHL22 and ATHB2 proteins were prepared as MBP fusions in E. coli cells (left panel, white arrows). The same amounts of proteins shown on the protein gel and 32P-labelled DNA fragments were used in the in vitro binding assays (middle panel). ATHB2-binding sequence was also assayed (right panel). kDa, kilodalton.

(B) Effects of core sequence mutations on AHL22 binding to *FT*-ATR. The core sequence of the AT-hook motif (RGRP) was mutated to RGAA, resulting in mAHL22 (upper panel). NTM1 and ATHB2 transcription factors were included as controls in the assays (lower panel).

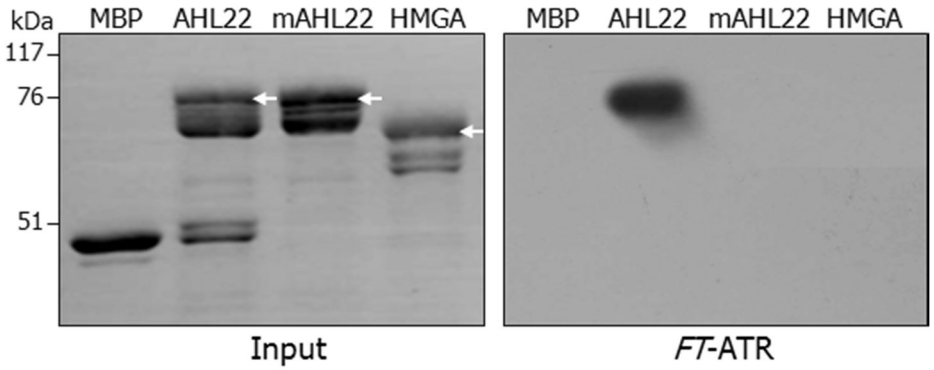

Figure 12. Binding of HMGA to FT-ATR.

Recombinant high mobility group A (HMGA) protein (At1g14900) was prepared as maltose binding protein (MBP) fusion in Escherichia coli cells in a similar manner with recombinant MBP-AHL22 fusion (left panel). White arrows indicate recombinant full-size MBP or MBP fusion proteins. The same amounts of proteins shown on the protein gel and 32P-labelled DNA fragments were used in the *in vitro* binding assays (right panel). The mutated AHL22 protein (mAHL22) was also included in the assays. kDa, kilodalton. Note that recombinant HMGA protein does not bind to *FT*-ATR.

To further examine the AHL22 binding to the *FT*-ATR, a mutated AHL22 protein (mAHL22) was synthesized by mutating the core RGRP sequence to RGAA within the AT-hook motif. The mAHL22 protein did not bind to the *FT*-ATR (Figure 11B, lower panel and Figure12), indicating that the interaction is mediated by the AT-hook, as has been shown with AHL1 (Fujimoto et al., 2004). Although ATHB2 bound to the *FT*-ATR, additional control transcription factors, such as NTM1 and its activated form ΔC that contain affinity for the *FT*-ATR, further supporting that the AHL22 binding to the *FT*-ATR is specific.

I next examined whether AHL22 binds to the *FT*-ATR in vivo, ChIP assays were carried out using 35S:*MYC-AHL22* transgenic plants that overexpress the *MYC-AHL22* gene fusion, in which a MYC-coding sequence was fused in-frame to the 5' end of the *AHL22* gene. Chromatin preparations extracted from the transgenic seedlings were probed with an anti-MYC antibody. Primer sets were designed so that PCR products of approximately 200bp, such as M1, M2, and M3 that cover different regions of the *FT*-ATR (Figure 13A), were synthesized. P1 is control DNA sequence region that covers 5' untranslated region and part of exon 1, to which the *FT* repressor TEMPRANILLO 1 (TEM1) binds (Castillejo and Pelaz, 2008).

Figure 13

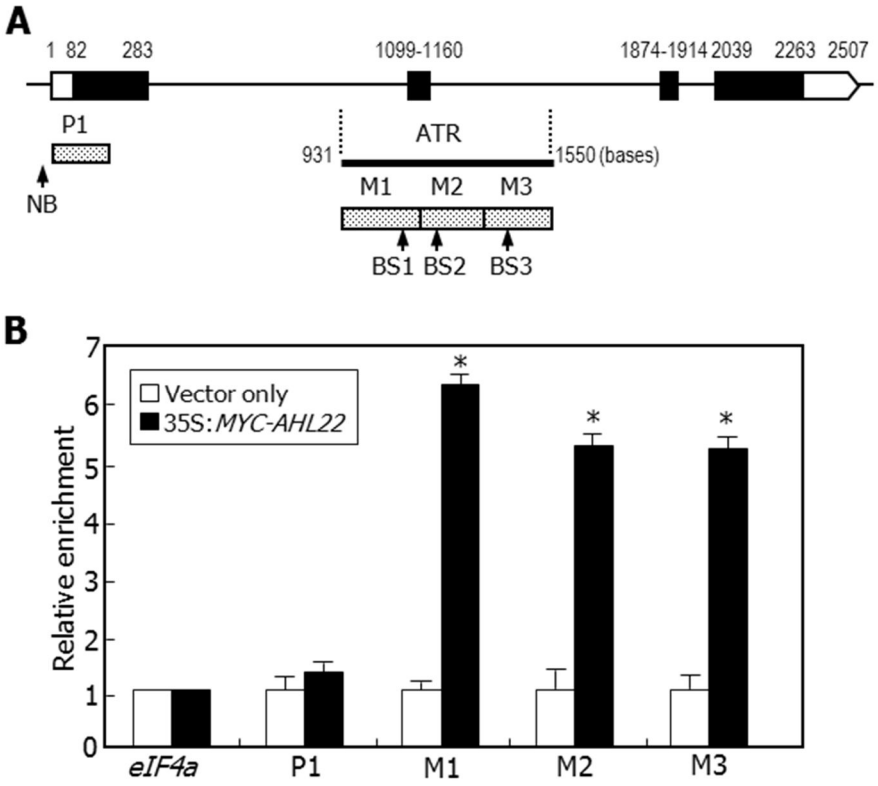
A
1 82 283
1099-1160
1874-1914 2039 2263 2507
P1
NB
931
ATR
1550 (bases)
M1 M2 M3
BS1 BS2 BS3
B
Vector only
35S:MYC-AHL22
Relative enrichment
0 1 2 3 4 5 6 7
*
*
*
eIF4a
P1
M1
M2
M3

Figure 13. Chromatin immunoprecipitation (ChIP) assays on AHL22 binding to *FT*-ATR.

(A) Location of ATR in *FT* locus. Black bars indicate exons, and white bars indicate untranslated regions. The *FT*-ATR was dissected into 3 sequence regions, M1 to M3. P1 is control DNA fragment. Putative binding sequences (BSs) of AHL22 were selected according to the rule proposed previously (Metcalf and Wassarman, 2006). NB, non-binding sequence.

(B) ChIP assays on AHL22 binding to *FT*-ATR. The 35S:*MYC-AHL22* transgenic plants grown on MS-agar plates for 2 weeks were used. Primer pairs specific to M1, M2, and M3 sequences were used. Three measurements were averaged and statistically treated (t-test, *P<0.01). Bars indicate standard error of the mean.

The assays using the primer sets covering the M1, M2, and M3 regions showed clear enrichment of the *FT*-ATR sequence, while those covering the P1 region did not show any enrichment of the *FT*-ATR sequence (Figure 13B). In addition, AHL22 binding to the M1 and M3 regions was further elevated in 35-day-old plants compared to that in 10-day-old plants (Figure 14), which is certainly due to the developmental stage-dependent activation of *FT* chromatin (Amasino, 2010). These observations demonstrate that AHL22 binding to the *FT*-ATR occurs in vivo.

An ATR sequence was also predicted in *AP1* and *LFY* locus (Figure 15A). AHL22 also bound to the intragenic ATR sequence in the *AP1* locus and the intergenic ATR sequence in the *LFY* locus (Figure 15B).

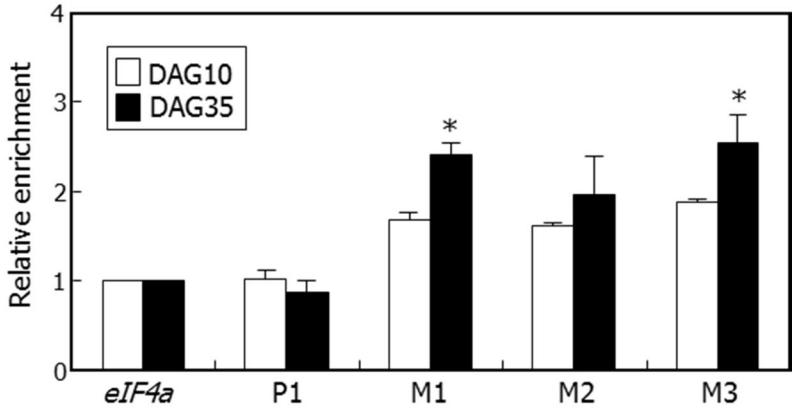

Figure 14. ChIP assays on kinetic binding of AHL22 to *FT*-ATR.

The 35S:*MYC-AHL22* transgenic plants that overexpress the *MYC-AHL22* gene fusion under the control of the Cauliflower Mosaic Virus (CaMV) 35S promoter, in which a MYC-coding sequence was fused in-frame to the 5' end of the *AHL22* gene, were grown on MS-agar plates under long days, and aerial plant parts were harvested 10 and 35 days after germination (DAG10 and DAG35, respectively). Primer pairs specific to M1, M2, and M3 sequences were used. Three measurements were averaged for each assay and statistically treated (t-test, *P<0.01). Bars indicate standard error of the mean. Note that relative enrichments of the *FT*-ATR sequence are higher 35 days after germination (DAG35) than at DAG10 in the M1 and M3 sequences.

Figure 15

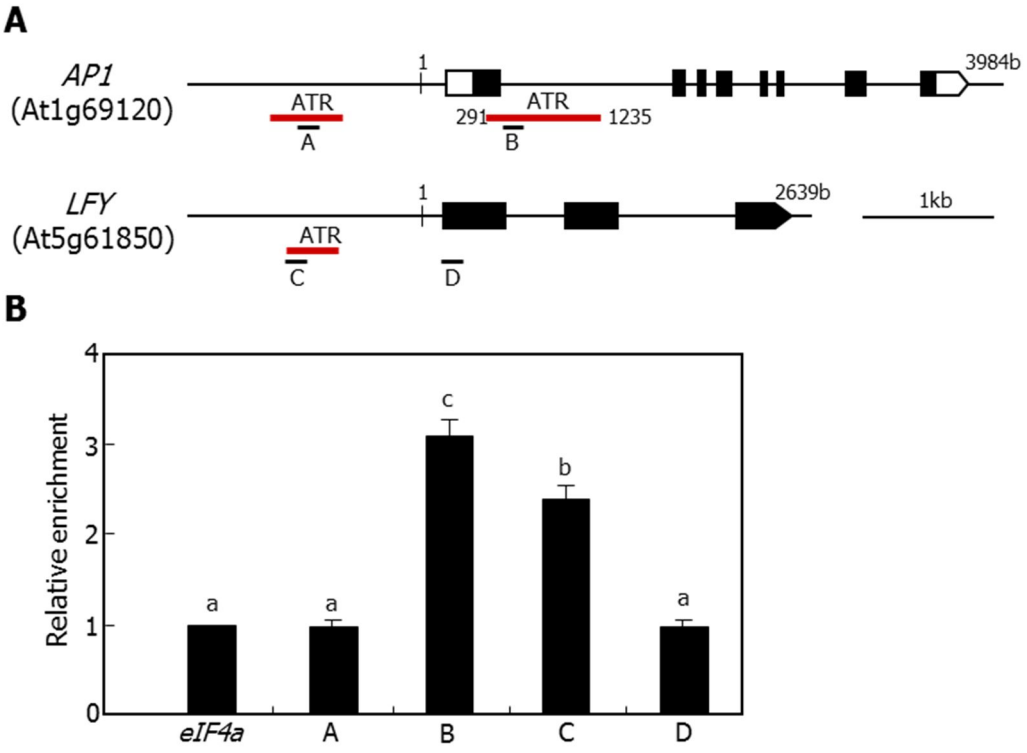
A
AP1
(At1g69120)
1
3984b
ATR
A
291
ATR
1235
B
LFY
(At5g61850)
1
2639b
1kb
ATR
C
D
B
Relative enrichment
0
1
2
3
4
a
a
c
b
a
eIF4a
A
B
C
D

Figure 15. ChIP assays on AHL22 binding to intergenic and intragenic ATRs of *AP1* and *LFY* loci.

(A) Prediction of ATRs in *AP1* and *LFY* loci.

Black bars indicate exons, and white bars indicate untranslated regions. Potential matrix attachment regions (MARs), which are characterized by stretches of AT-rich sequences (ATRs) [Rudd, S., Frisch, M., Grote, K., Meyers, B. C., Mayer, K., and Werner, T. (2004) Plant Physiol. 135, 715-722], were predicted using the SMARTest software (http://www.genomatrix.de). One intragenic ATR was predicted in *AP1* locus as in *FT* locus. The intragenic *AP1*-ATR includes parts of exon 1 and intron 1 and consists of 945 nucleotides. Note that there is no intragenic ATR in *LFY* locus. b, bases. kb, kilobases. One intergenic ATR, which is closest to the transcriptional start site, was indicated for each of *AP1* and *LFY* loci. Sequence regions, marked by A – D, were chosen for ChIP assays.

(B) ChIP assays on AHL22 binding to *AP1* and *LFY*-ATRs. The 35S:*MYC*-*AHL22* transgenic plants grown on MS-agar plates for 35 days were used. Primer pairs specific to the sequences (A–D) were used. Three measurements were averaged and statistically treated. Different letters represent significant difference at $P<0.05$ (one-way ANOVA with Fisher's post hoc test). Bars indicate standard error of the mean.

I also carried out EMSA assays using DNA sequences bearing AAT, ATT, TAA and TTA within the *FT*-ATR as probes (Figure 16, upper panel). The DNA fragments of approximately 20 nucleotides containing the consensus motifs were end-labelled, and their binding to recombinant MBP-AHL22 fusion protein was assayed. It was found that AHL22 bound strongly to the binding sequences (BSs) that are homologous to the *FT*-ATR (Figure 16, lower panel). In addition, the AHL22 binding was significantly reduced in the presence of excess unlabelled BS fragments but only slightly reduced in the presence of mutated DNA fragments (mBSs), supporting the specific binding of AHL22 to the BS sequences. In contrast, I did not detect any detectable binding of mAHL22 to the BS sequences.

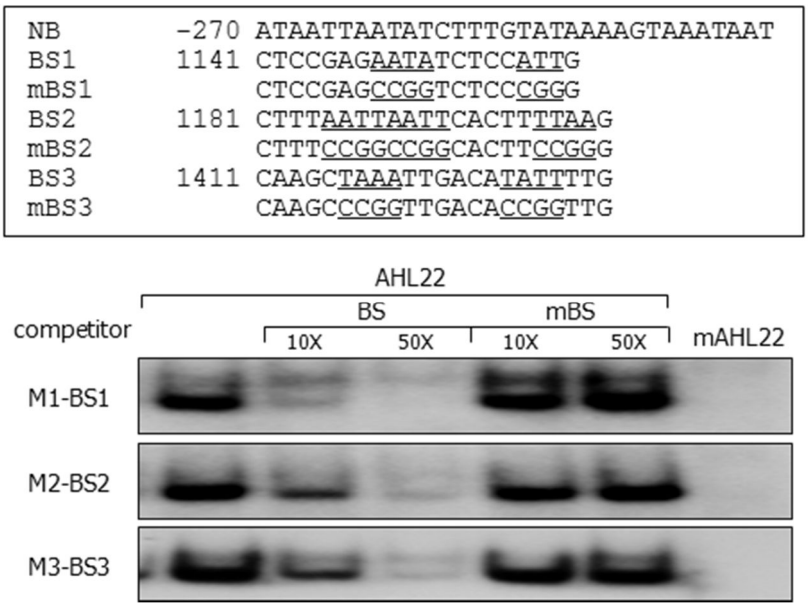

Figure 16. EMSA assays on AHL22 binding to *FT*-ATR.

EMSA assays on AHL22 binding to *FT*-ATR. The BS sequences were mutated to verify specific binding, resulting in mBS sequences (upper panel). Increasing amounts of unlabelled BS or mBS oligonucleotides were added to the assay mixtures (lower panel).

4. 5. Effects of AT-Hook mutation on AHL22 function in flowering

I next examined whether AHL22 binding to the *FT*-ATR is physiologically important in flowering. To examine this, the *mAHL22* gene was overexpressed in *Arabidopsis*. Unlike the late-flowering 35S:*AHL22* transgenic plants, the 35S:*mAHL22* transgenic plant did not exhibit late flowering (Figure 17A). qRT-PCR assays revealed that the *mAHL22* transcript level in the 35S:*mAHL22* transgenic plant was similar to that in the OE-*AHL22 mutant* (Figure 17B, left panel). In contrast, the *FT* transcript level was not reduced in the 35S:*mAHL22* transgenic plant, which was in contrast to the significant suppression of the *FT* gene in the OE-*AHL22* mutant (Figure 17B, right panel). These observations indicate that the AHL22 binding to the *FT*-ATR is linked with the AHL22-mediated delaying flowering.

Based on the specific binding of AHL22 to the *FT*-ATR, it was predicted that AHL22 would be localized in the nucleus. I examined the subcellular localization of AHL22 using transgenic plants overexpressing a GFP-AHL22 fusion, in which a GFP-coding sequence was fused in-frame to the 5' end of the *AHL22* gene. The assays showed that AHL22 is localized exclusively in the nucleus (Figure 18A). The mAHL22 protein was also localized in the nucleus, indicating that the AT-hook motif is not essential for the nuclear localization of AHL22.

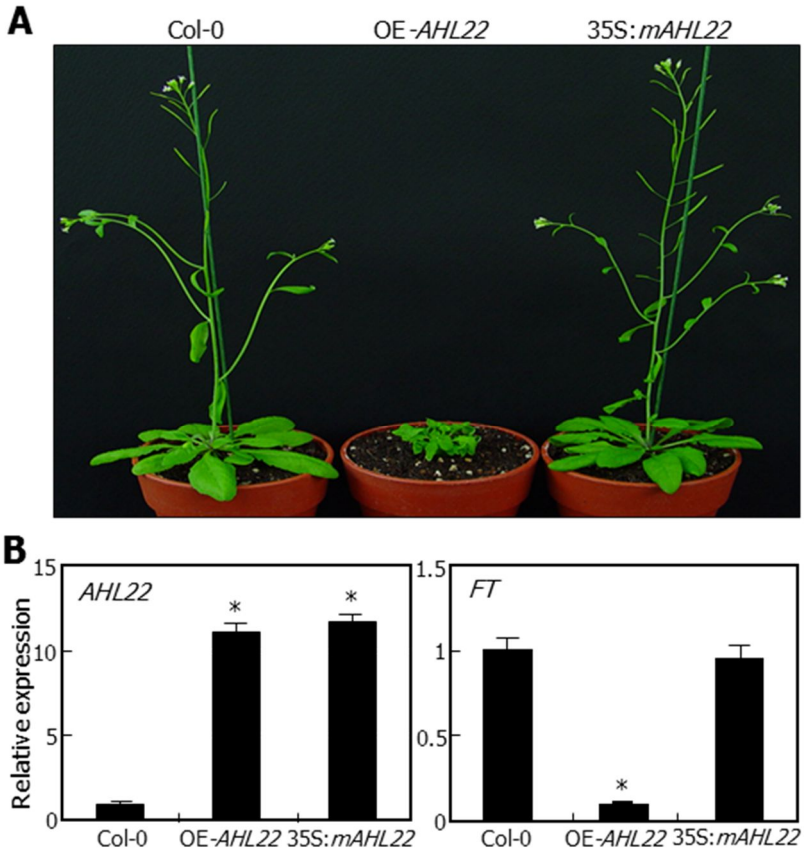

Figure 17. Effects of AHL22 mutation on *FT* expression and flowering.

(A) Flowering phenotypes of 35S:mAHL22 transgenic plants.

(B) Relative transcript levels of *FT* and AHL22 genes. Two-week-old whole plants grown on MS-agar plates were used for extraction of total RNA. Transcript levels were determined by qRT-PCR. Biological triplicates were averaged and statistically treated (t-test, *P<0.01). Bars indicate standard error of the mean.

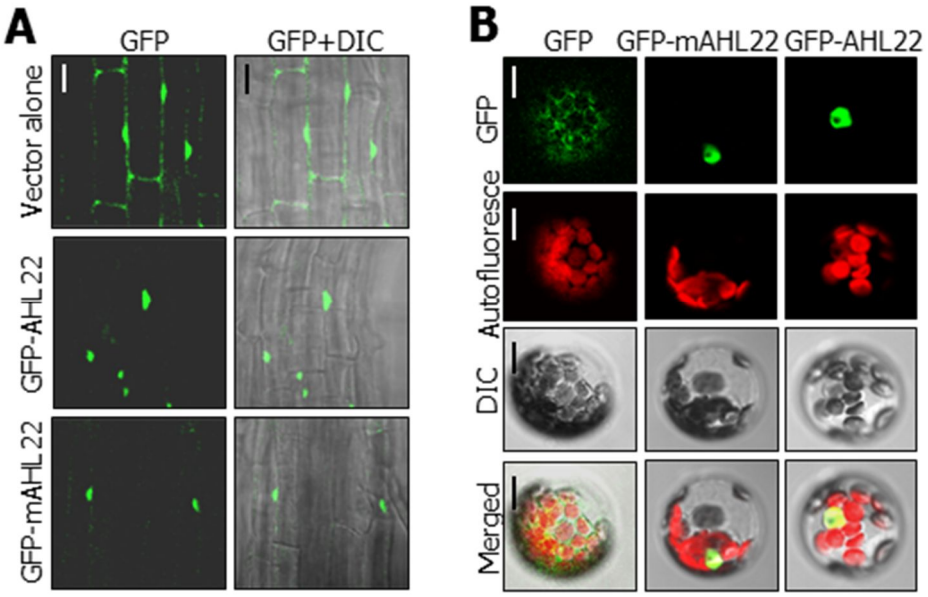

Figure 18. Subcellular localization of AHL22 proteins.

(A) Nuclear localization of AHL22 protein in roots.

(B) Nuclear localization of AHL22 protein in *Arabidopsis* protoplasts. The *GFP-AHL22* and *GFP-mAHL22* gene fusions were either transformed into Col-0 plants (A) or transiently expressed in *Arabidopsis* protoplasts (B). In (A), root samples were visualized by differential interference contrast microscopy (DIC) and fluorescence microscopy. Scale bar, 40 μm. In (B), *Arabidopsis* protoplasts were examined by confocal microscopy. Scale bar, 10 μm.

The subcellular distribution of the AHL22 and mAHL22 proteins was further examined by transiently expressing the GFP-AHL22 and GFP-mAHL22 fusions in *Arabidopsis* protoplasts. Both the AHL22 and mAHL22 proteins were localized exclusively in the nucleus (Figure 18B), demonstrating that the AHL22 protein is localized in the nucleus, where it binds to the *FT*-ATR.

4. 6. AHL22 suppression of *FT* in flowering

These data showed that AHL22 suppresses *FT* expression by binding directly to the *FT*-ATR. Therefore, a question was whether the AHL22 suppression of *FT* is physiologically important in flowering.

To address the question, I produced two independent transgenic plants: one overexpressing genomic *FT* gene sequence (*gFT*) and the other overexpressing *FT* cDNA (*cFT*). The *gFT* gene consisting of 2180 bp included four exons and three introns (Figure 19A). It also included the *FT*-ATR. In contrast, the *cFT* gene consisting of 528 bp lacks intact *FT*-ATR, and thus AHL22 is unable to bind to the *FT* cDNA. The 35S:*gFT* and 35S:*cFT* transgenic plants were also genetically crossed with the late-flowering OE-*AHL22* mutant, resulting in 35S:*gFT* OE-*AHL22* and 35S:*cFT* OE-*AHL22* plants.

Both the 35S:*gFT* and 35S:*cFT* transgenic plants flowered very early at the rosette leaf number (RLN) of 2.1 ± 0.3 and 4.6 ± 0.5, respectively (Figure 19B). The *FT* transcript levels were accordingly elevated drastically in the transgenic plants (Figure 19C). The 35S:*gFT* OE-*AHL22* and 35S:*cFT* OE-*AHL22* plants also exhibited early flowering (Figure 19B).

However, counting of RLN revealed that the early-flowering phenotype of the 35S:*gFT* transgenic plants was detectably repressed in the 35S:*gFT* OE-*AHL22* plants, which flowered at the RLN of 4.8 ± 0.6. In contrast, the early-flowering phenotype of the 35S:*cFT* transgenic plants were suppressed only slightly in the 35S:*cFT* OE-*AHL22* transgenic plants, which flowered at the RLN of 5.6 ± 0.5.

Consistent with the changes in flowering times, the *FT* transcript level was detectably reduced in the 35S:*gFT* OE-*AHL22* plants compared to that in the 35S:*gFT* transgenic plants (Figure 19C). In contrast, the *FT* transcript level in the 35S:*cFT* OE-*AHL22* plants was largely unchanged compared to that in the 35S:*cFT* transgenic plants, which is certainly because the *FT* cDNA is not targeted by AHL22. These observations demonstrate that AHL22 regulates flowering time by modulating *FT* expression.

Figure 19

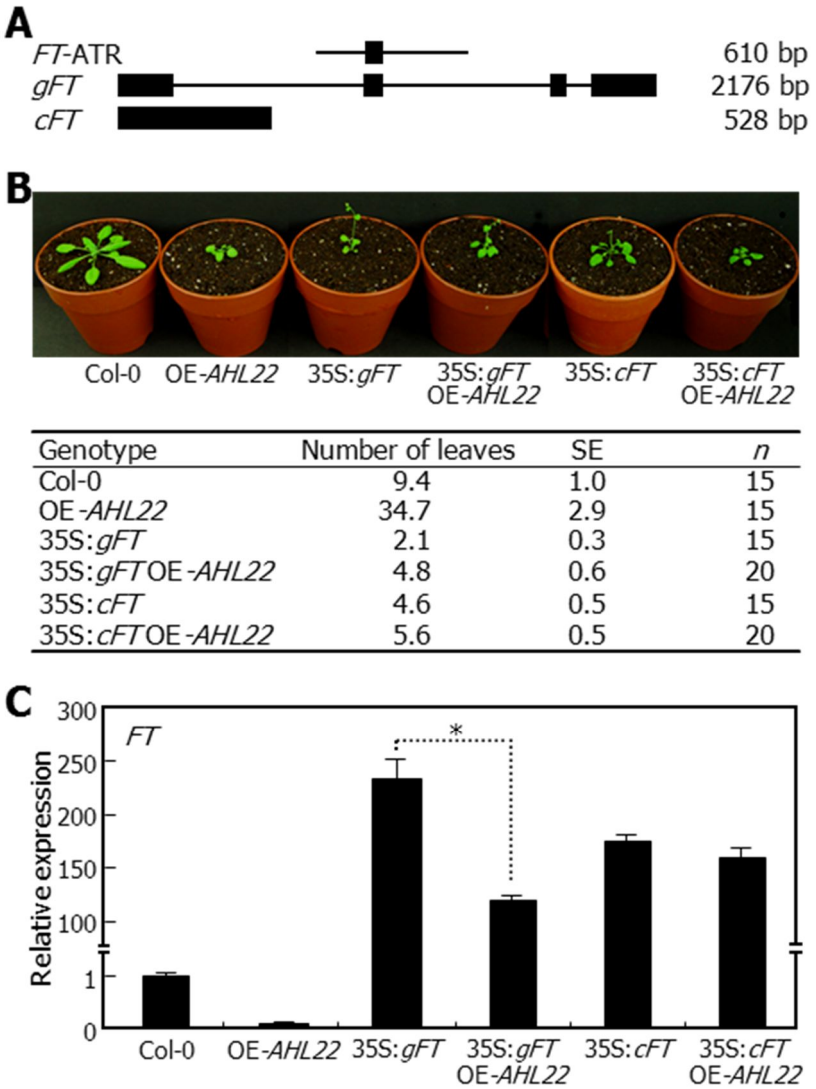

Genotype	Number of leaves	SE	*n*
Col-0	9.4	1.0	15
OE-*AHL22*	34.7	2.9	15
35S:*gFT*	2.1	0.3	15
35S:*gFT* OE-*AHL22*	4.8	0.6	20
35S:*cFT*	4.6	0.5	15
35S:*cFT* OE-*AHL22*	5.6	0.5	20

Figure 19. AHL22 suppression of *FT* gene in flowering.

(A) *FT* gene constructs used. Black boxes indicate exons. bp, base pair.

(B) Flowering phenotypes of transgenic plants overexpressing either *gFT* or *cFT* sequence. Four-week-old plants grown in soil under LDs were photographed (upper panel). Flowering times were measured by counting rosette leaf numbers at bolting (lower panel). Fifteen to twenty plants were counted and averaged for each plant genotype. Values are mean ± standard error (SE).

(C) *FT* transcript levels. Whole plants grown on MS-agar plates for 10 days under LDs were used for extraction of total RNA. Transcript levels were determined by qRT-PCR. Biological triplicates were averaged and statistically treated (t-test, *P<0.01). Bars indicate standard error of the mean.

4. 7. AHL22 regulation of H3 acetylation and methylation in *FT* chromatin

Recent studies have shown that some AT-hook proteins function in chromatin remodeling in both animals and plants (Aravind and Landsman, 1998). MAR-binding factors play a role in gene regulation by mediating chromatin modifications (Tetko et al., 2006; Reeves, 2010). These data showed that AHL22 interacts with the *FT*-ATR, which has been suggested to act as an intragenic MAR (Rudd et al., 2004). I therefore examined whether the AHL22 repression of *FT* transcription is mediated by histone modifications.

I carried out ChIP assays on the *FT* chromatin using the primer sets used in the ChIP assays on AHL22 binding to *FT*-ATR (Figure 13A). The ChIP assays revealed that H3 acetylation (H3Ac), which is a mark for active gene expression (Santos-Rosa et al., 2002), was reduced approximately 70% in the *FT*-ATR in the OE-*AHL22* mutant compared to that in Col-0 plants (Figure 20A). In contrast, H3 dimethylation at Lys-9 (H3K9me2), a repressive mark for gene expression (Litt et al., 2001), increased approximately ~2-fold in the mutant (Figure 20B). These observations indicate that AHL22 modulates the *FT* chromatin within the *FT*-ATR by modulating H3 acetylation and Lys-9 dimethylation.

Figure 20

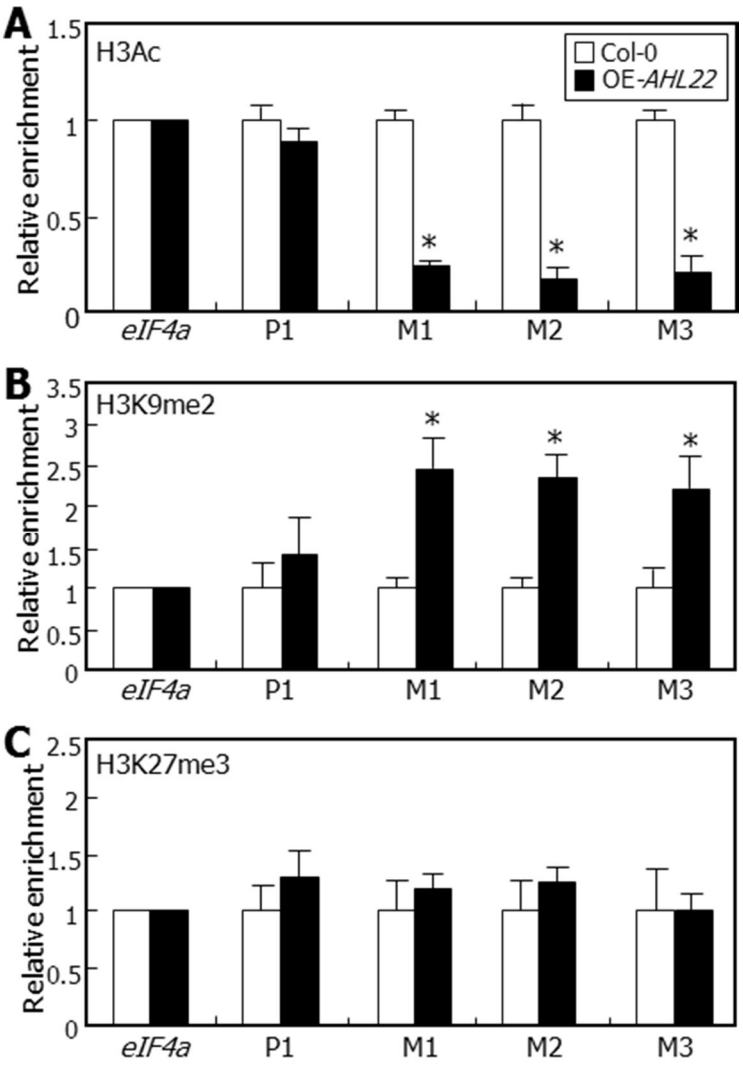
A
H3Ac
Col-0
OE-AHL22
Relative enrichment
1.5
1
0.5
0
*
*
*
eIF4a
P1
M1
M2
M3
B
H3K9me2
Relative enrichment
3.5
3
2.5
2
1.5
1
0.5
0
*
*
*
eIF4a
P1
M1
M2
M3
C
H3K27me3
Relative enrichment
2.5
2
1.5
1
0.5
0
eIF4a
P1
M1
M2
M3

Figure 20. Modifications of *FT* chromatin by AHL22.

Relative levels of H3 modifications in *FT* chromatin were examined by ChIP assays using an anti-H3Ac (A), -H3K9me2 (B), or -H3K27me3 (C) antibody. PCR primer pairs specific to M1, M2, and M3 sequences, as shown in Figure 2A, were used. Plants grown on MS-agar plants for 12 days under LDs were used for chromatin preparations. Three measurements were averaged and statistically treated (t-test, *P<0.01). Bars indicate standard error of the mean.

In contrast, H3 trimethylation at Lys-27 (H3K27me3), which is another repressive mark for gene expression (Kirmizis et al., 2004), was not changed to a discernible level in the mutant (Figure 20C), suggesting that H3K27me3 is not involved in the AHL22-mediated modifications of the *FT* chromatin.

4. 8. Interactions of AHL22 with HDACs

Histone deacetylases (HDACs) are a group of enzymes that remove acetyl groups from acetylated Lys residues of histone proteins (Hollender and Liu, 2008). I found that H3 acetylation is reduced in the *FT* chromatin of the OE-*AHL22* mutant. I therefore asked whether the AHL22-mediated modifications of the *FT* chromatin are related with HDACs.

I first carried out *in vitro* pull-down assays using recombinant MBP-AHL22 fusion protein and *in vitro* translated HDAC polypeptides to examine whether AHL22 interacts with HDAC enzymes. It was found that AHL22 strongly interacted with HDA1/HDA19, HDA6, and HDA9 (Figure 21A), which are involved in flowering timing and floral architecture (Hollender and Liu, 2008). The three HDAC proteins did not bind to MBP alone, supporting the specific interaction between the HDAC enzymes and AHL22 protein.

I also carried out BiFC assays to further examine the AHL22-HDAC interactions. The nYFP- and cYFP-coding sequences were fused in-frame to

the 5' and 3' ends of the *AHL22* and *HDAC* gene sequences, and the fusion constructs were coexpressed transiently in *Arabidopsis* protoplasts.

Strong reconstituted YFP signals were detected in the nuclei of cells coexpressing the AHL22-nYFP and HDAC-cYFP fusions and the AHL22-cYFP and HDAC-nYFP fusions (Figure 21B), confirming that AHL22 interacts with the HDAC enzymes in the nucleus.

Dynamic dimer formation regulates the binding specificity and affinity of transcription regulators to their target DNA or interacting partners (Vinson et al., 2006). I therefore examined whether AHL22 forms homodimers by *in vitro* pull-down assays using recombinant MBP-AHL22 proteins and [35S] methionine-labelled AHL22 polypeptides. I found that the two AHL22 forms interact with each other (Figure 22A). In addition, BiFC assays in *Arabidopsis* protoplasts showed that the two AHL22 forms interact with each other *in vivo* (Figure 22B). Notably, the mAHL22 protein also interacts with AHL22 in both *in vitro* pull-down assays and BiFC assays (Figure 22A and 22B), indicating that the AT-hook motif is not required for the interactions. These observations support that the AHL22 proteins form multimers, probably homodimers.

Figure 21

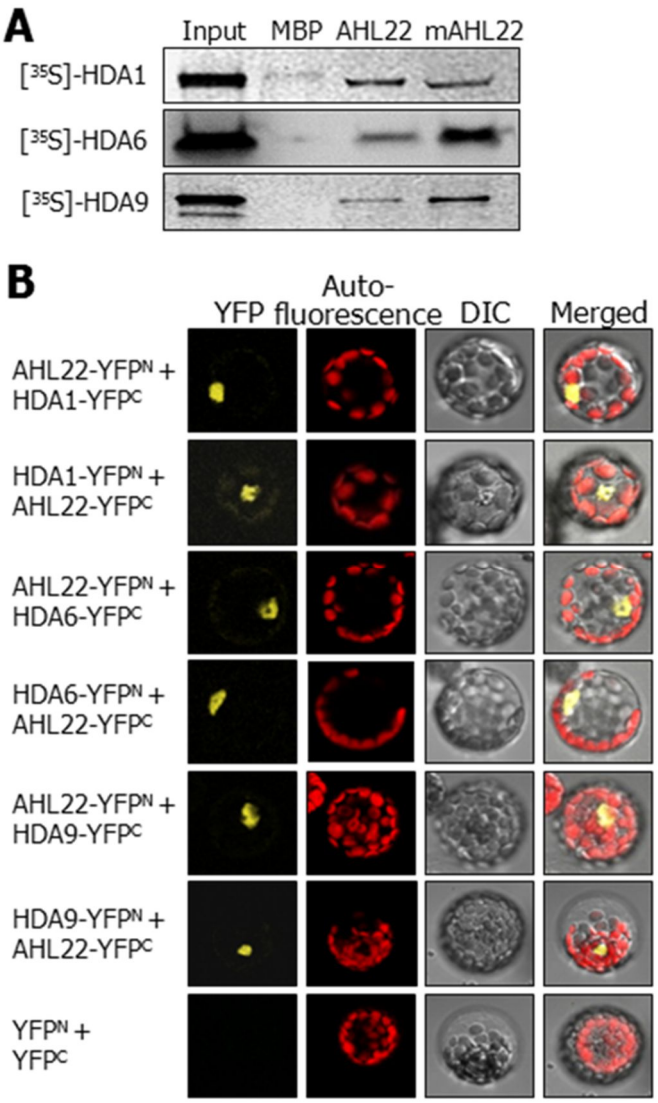
A
Input
MBP
AHL22
mAHL22
[35S]-HDA1
[35S]-HDA6
[35S]-HDA9
B
Auto-
YFP fluorescence
DIC
Merged
AHL22-YFPN + HDA1-YFPC
HDA1-YFPN + AHL22-YFPC
AHL22-YFPN + HDA6-YFPC
HDA6-YFPN + AHL22-YFPC
AHL22-YFPN + HDA9-YFPC
HDA9-YFPN + AHL22-YFPC
YFPN + YFPC

Figure 21. Interaction of AHL22 with HDACs.

(A) *in vitro* pull-down assays. [35S]-labelled HDAC polypeptides were prepared by *in vitro* translation. Recombinant MBP-AHL22 and MBP-mAHL22 proteins prepared in E. coli cells were used. Input represents 5% of the HDAC protein used in each assay.

(B) BiFC assays in *Arabidopsis* protoplasts. The cYFP and nYFP fusions were cotransfected into *Arabidopsis* protoplasts and visualized by differential interference contrast microscopy (DIC) and fluorescence microscopy. Scale bar, 10 m.

Figure 22

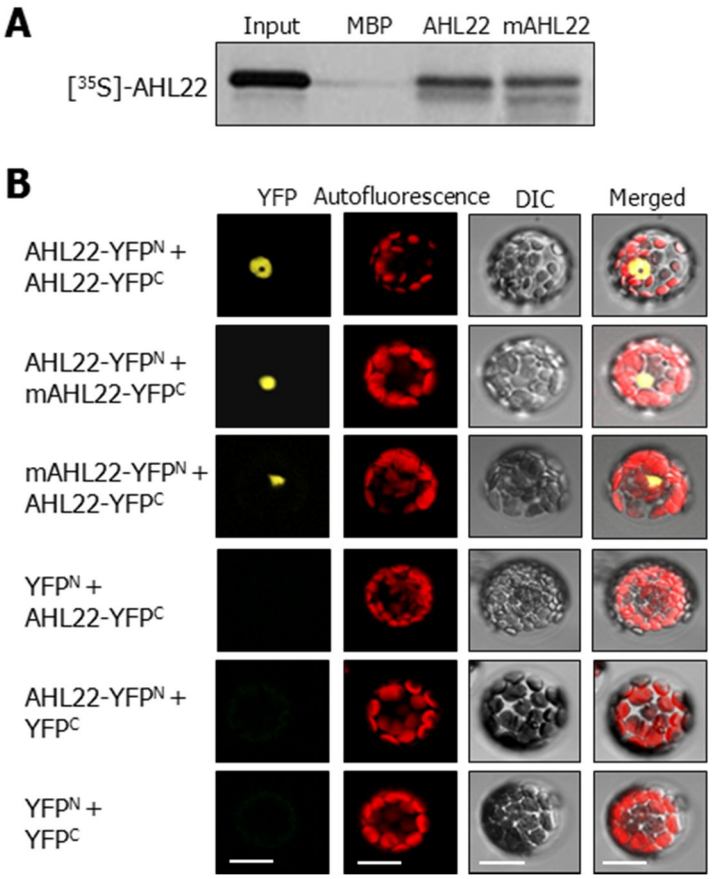
A
Input
MBP
AHL22
mAHL22
[35S]-AHL22
B
YFP
Autofluorescence
DIC
Merged
AHL22-YFPN + AHL22-YFPC
AHL22-YFPN + mAHL22-YFPC
mAHL22-YFPN + AHL22-YFPC
YFPN + AHL22-YFPC
AHL22-YFPN + YFPC
YFPN + YFPC

Figure 22. AHL22-AHL22 interactions *in vitro* and in *Arabidopsis* protoplasts.

(A) *in vitro* pull-down assays. *in vitro* translated, [35S]methionine-labelled AHL22 polypeptides were pulled down with recombinant MBP-AHL22 fusion protein prepared in E. coli cells. mAHL22, in which the core sequence of the AT-hook motif (RGRP) was mutated to RGAA, was similarly prepared as MBP-mAHL22 fusion in E. coli cells. Input represents 5% of the protein sample used in each assay.

(B) Bimolecular fluorescence complementation (BiFC) assays in *Arabidopsis* protoplasts. The cYFP and nYFP fusions were cotransformed into *Arabidopsis* protoplasts and visualized by differential interference contrast microscopy (DIC) and fluorescence microscopy. Scale bar, 10 mm.

I next examined whether HDAC activity is important for *FT* regulation by employing trichostatin A (TSA) that selectively inhibits class I and II mammalian HDAC enzymes (Vinson et al., 2006). *Arabidopsis* plants were grown for 10 days on MS-agar plates containing 0.5 μM TSA, and *FT* transcript levels were examined. The *FT* transcript level was elevated at least 7-fold in the TSA-treated OE-*AHL22* mutant (Figure 23). In contrast, the AHL22 transcription was not affected by TSA under identical conditions, indicating that HDACs participate in the AHL22-mediated suppression of *FT* transcription.

Altogether, these data demonstrate that the AHL22 protein suppresses *FT* transcription by binding to the *FT*-ATR and recruiting a subset of HDAC enzymes. A plausible working scenario is that the AHL22-HDAC complexes deacetylate acetylated histones in the *FT* chromatin (Figure 24). AHL22 also regulates H3 dimethylation at Lys-9, suggesting that histone methyltransferases (HMTases) are also involved in the AHL22-mediated modification of the *FT* chromatin.

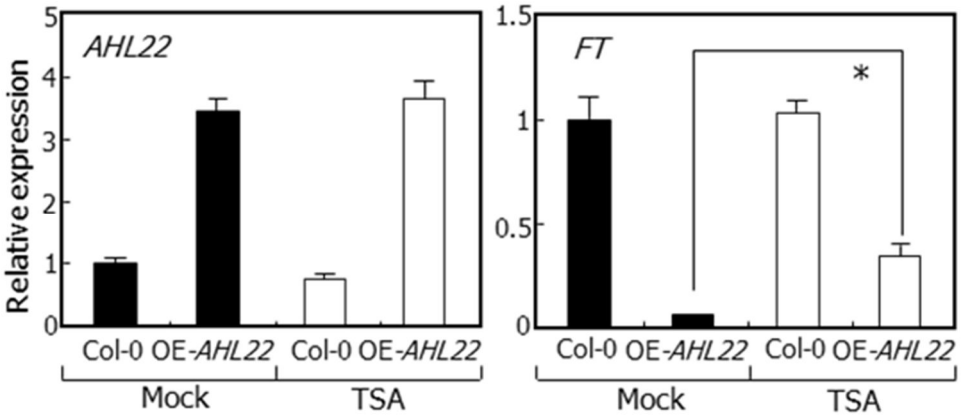

Figure 23. Effects of TSA on *FT* expression in OE-*AHL22* mutant.

Transcript levels were determined by qRT-PCR. Biological triplicates were averaged and statistically treated using a student t-test (*P<0.01). Bars indicate standard error of the mean.

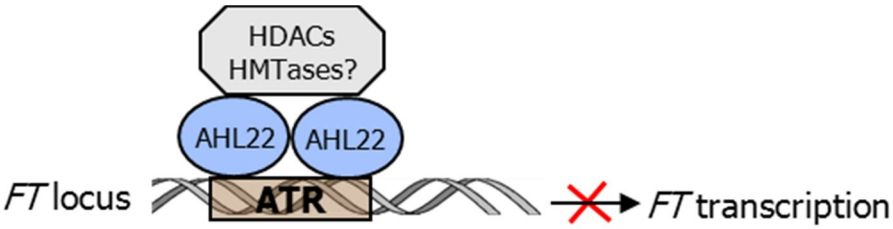

Figure 24. Schematic model of AHL22 function in flowering.

The AHL22 protein suppresses *FT* transcription by binding to the *FT*-ATR and recruiting a subset of HDAC enzymes. The AHL22-HDAC complexes deacetylate acetylated histones in the *FT* chromatin. AHL22 also regulates H3 dimethylation at Lys-9, suggesting that histone methyltransferases (HMTases) are also involved in the AHL22-mediated modification of the *FT* chromatin.

V. DISCUSSION

The AHL proteins are characterized by having two conserved structural components: the AT-hook motif that binds to AT-rich stretches of DNA and the plant and prokaryotic conserved (PPC) domain that mediate nuclear localization (Fujimoto et al., 2004). Several AHL proteins have been functionally studied in diverse aspects of plant growth and developmental processes and stress responses in *Arabidopsis*. AGF1/AHL25 is critical for the negative feedback regulation of GA3 oxidase gene (Matsushita et al., 2007). SOB3/AHL29 and ESC/ORE7/AHL27 are known to regulate hypocotyl growth (Street et al., 2008). It also acts as a negative regulator of leaf senescence (Lim et al., 2007). In addition, GIK/AHL21 plays a role in organ patterning and differentiation (Ng et al., 2009).

Furthermore, it has been reported that AHL22 is involved in flowering induction and hypocotyl elongation (Xiao et al., 2009). Meanwhile, overexpression of *AHL20* gene suppresses plant innate immune responses (Lu et al, 2010). AHL15, AHL19, and AHL27 have also been implicated in defence responses (Lu et al, 2010).

It is notable that AHL1 binds to MARs via the AT-hook motif (Fujimoto et al., 2004). MARs are specific stretches of DNA sequences that are important for the structural organization of chromatin fibers by anchoring

chromatin loops to nuclear matrix (Rudd et al., 2004). A genome-scale study of gene expression patterns in conjunction with screening of potential intragenic MARs has shown that *Arabidopsis* genes possessing intragenic MARs tend to be less expressed irrespective of plant tissues and organs and differentially regulated throughout the plant growth stages (Rudd et al., 2004; Tetko et al.,2006). It has been known that MARs link AHL proteins with chromatin modifications. For example, ESC/ORE7/AHL27 influences chromatin architecture by modulating the distribution of H2B (Lim et al., 2007). In addition, AHL21 represses *AUXIN RESPONSE FACTOR 3* (*ARF3*) gene by inducing H3 dimethylation at Lys-9 in the gene promoter during floral development (Ng et al., 2009).

In this work, I demonstrated that AHL22 suppresses *FT* expression by binding to the *FT*-ATR and recruiting a subset of HDAC enzymes, HDA1/HDA19, HDA6, and HDA9. The early-flowering phenotype of the 35S:*gFT* transgenic plants was compromised in the OE-*AHL22* background (35S:*gFT* OE-*AHL22*). Consistent with the changes in flowering time, *FT* transcript level was reduced in the 35S:gFT OE-AHL22 plants compared to that in the 35S:*gFT* transgenic plants. In contrast, the early-flowering phenotype of the 35S:*cFT* transgenic plants was reduced only slightly in the OE-*AHL22* background (35S:*cFT* OE-*AHL22*), which is obviously because the *FT* cDNA does not have intact *FT*-ATR to which AHL22 binds.

The *FT*-ATR has been predicted as an intragenic MAR (Rudd et al., 2004). A major group of MAR-binding factors possesses the AT-hook motif (Aravind and Landsman, 1998). AHL1 is associated with the nuclear matrix (Fujimoto et al., 2004). It is therefore likely that AHL22 acts as a MAR-binding factor in *Arabidopsis*.

These data strongly support that AHL22 regulates *FT* expression by modulating histone acetylation and methylation through physical interactions with HDACs and presumably methyltransferase enzymes. Whereas the level of H3Ac was reduced, that of H3K9me2 was elevated in the *FT* chromatin of the late-flowering OE-*AHL22* mutant, while H3K27 trimethylation may not be involved in *FT* control (Figure 20). The physiological significance of the AHL22-HDAC interactions in *FT* regulation and thus flowering time control is further supported by the effects of the HDAC inhibitor TSA on *FT* expression in the OE-*AHL22* mutant. However, the role of the AHL22-HDAC interactions in flowering time control likely is more complicated than the proposed working model (Figure 24). AHL proteins are functionally redundant, and at least several AHL proteins are apparently involved in flowering time control (Street et al., 2008; Xiao et al., 2009; Lu et al, 2010), suggesting that different AHL proteins may interact with different HDAC enzymes. This view entails that various combinations of AHL-HDAC

complexes would bind to the *FT*-ATR, depending on developmental and environmental signals.

I observed that *LFY* and *AP1* genes, in addition to *FT*, are also suppressed in the OE-*AHL22* mutant (Figure 6B). In addition, AHL22 bound to the intragenic and intergenic ATR sequences in the *AP1* and *LFY* loci, respectively. It is therefore likely that the AHL22-HDAC complexes also regulate the chromatin status of *LFY* and *AP1* genes and other flowering time genes in addition to *FT* gene. This signalling complexity may explain the relatively small changes of *FT* transcript levels and the timing of flowering initiation observed in the 35S:*gFT* OE-*AHL22* plants compared to those in the 35S:*gFT* transgenic plants. Further work is necessary to determine how much the AHL22-HDAC regulation of *FT* chromatin contributes to the role of *FT* in flowering time control. In addition, the role of endogenous and environmental factors in regulating AHL22 activity should also be investigated.

Coordinated histone modifications mediate epigenetic regulation of gene expression in plants. One of the most extensively studied is epigenetic regulation of the floral repressor *FLC*. It has been known that epigenetic regulation of the *FLC* gene is mediated by complex networks of histone acetylation and methylation events. Activation of the *FLC* expression is achieved through several active chromatin modifications, such as acetylation of core histone tails, H3K4 methylation, and H3K36 dimethylation and

trimethylation (He, 2009). In contrast, repressive histone modifications, including histone deacetylation, H3K4 demethylation, H3K9 and H3K27 methylation, and histone arginine methylation, repress the *FLC* expression (He, 2009).

Histone modifications in *FT* chromatin have recently been studied. Whereas H3K4 trimethylation in the *FT* chromatin is associated with *FT* activation, H3K27 trimethylation is associated with *FT* repression. It has been found that the H3K27 methyltransferase CURLY LEAF (CLF) represses *FT* expression (Jiang et al., 2008). In addition, the chromodomain-containing LIKE HETERO CHROMATIN PROTERIN 1 (LHP1) protein binds to H3K27me3 in the *FT* chromatin and maintains the repressive state of *FT* expression (Turck et al., 2007). However, there is little known about the role of histone acetylation/deacetylation in the *FT* chromatin. I found that AHL22 binds to an AT-rich DNA sequence in the *FT* locus and reduces H3 acetylation. I also found that H3 dimethylation at K9 is elevated in the *FT* chromatin of the OE-*AHL22* mutant. It seems that the *FT* chromatin is regulated through coordinated actions of histone acetylation and methylation, although not precisely in the way that epigenetic modifications control *FLC* gene.

HDAC enzymes play a role in global gene repression during developmental processes and stress adaptation responses in plants (Hollender

and Liu, 2008). AHL22 physically interacts with HDA1/HDA19, HDA6, and HDA9, which are homologous to yeast RPD3 (reduced potassium deficiency 3) and belong to type I HDAC subfamily (Hollender and Liu, 2008). In Saccharomyces pombe, mutations in the subunits of class I HDAC complexes affect H3K9 methylation (Silverstein et al., 2003), indicating that K9 deacetylation is a prerequisite for subsequent H3 methylation. I found that H3K9 dimethylation was elevated in the *FT* chromatin of the OE-*AHL22* mutant. Based on the previous and these data, I believe that AHL22 regulates the *FT* chromatin in a similar manner to the yeast RPD3: H3 deacetylation by HDAC enzymes may precede H3K9 dimethylation to suppress *FT* expression. In this view, it is envisaged that AHL22 may also interact with histone methyltransferases (Figure 24).

VI. REFERENCES

Abe, M., Kobayashi, Y., Yamamoto, S., Daimon, Y., Yamaguchi, A., Ikeda, Y., Ichinoki, H., Notaguchi, M., Goto, K., and Araki, T. (2005) FD, a bZIP protein mediating signals from the floral pathway integrator *FT* at the shoot apex. Science **309**, 1052–1056

Ahmada, A., Zhanga, Y., and Cao, X. (2010) Decoding the Epigenetic Language of Plant Development. Mol. Plant **3**, 719–728

Alen, C., Kent, N. A., Jones, H. S., O'Sullivan, J., Aranda, A., and Proudfoot, N. J. (2002) A role for chromatin remodeling in transcriptional termination by RNA polymerase II. Mol. Cell **10**, 1441–1452

Allen, G. C., Spiker, S., and Thompson, W. F. (2000) Use of matrix attachment regions (MARs) to minimize transgene silencing. Plant Mol. Biol. **43**, 361-376

Amasino, R. (2010) Seasonal and developmental timing of flowering. Plant J. **61**, 1001–1013

An, H., Roussot, C., Suárez-López, P., Corbesier, L., Vincent, C., Piñeiro, M., Hepworth, S., Mouradov, A., Justin, S., Turnbull, C., and Coupland, G. (2004) CONSTANS acts in the phloem to regulate a

systemic signal that induces photoperiodic flowering of *Arabidopsis*. Development **131**, 3615–3626

Aravind, L., and Landsman, D. (1998) AT-hook motifs identified in a wide variety of DNA-binding proteins. Nucleic Acids Res. **26**, 4413–4421

Ausin, I., Alonso-Blanco, C., Jarillo, J. A., Ruiz-Garcia, L., and Martinez-Zapater, J. M. (2004) Regulation of flowering time by FVE, a retinoblastoma-associated protein. Nat. Genet. **36**, 162–166

Balasubramanian, S., Sureshkumar, S., Lempe, J., Weigel, D. (2006) Potent induction of *Arabidopsis thaliana* flowering by elevated growth temperature. PLoS Genet. **2**, e106

Bastow, R., Mylne, J. S., Lister, C., Lippman, Z., Martienssen, R. A., and Dean, C. (2004) Vernalization requires epigenetic silencing of *FLC* by histone methylation. Nature **427**,164–167

Blázquez, M. A., Ahn, J. H., and Weigel, D. (2003) A thermosensory pathway controlling flowering time in *Arabidopsis thaliana*. Nat. Genet. **33**, 168–171

Blázquez, M. A., and Weigel, D. (2000) Integration of floral inductive signals in *Arabidopsis*. Nature **404**, 889–892

Blázquez, M. A., Green, R., Nilsson, O., Sussman, M. R., and Weigel, D. (1998) Gibberellins promote flowering of *Arabidopsis* by activating the LEAFY promoter. Plant Cell **10**, 791–800

Bode, J., Stengert-Iber, M., Kay, V., Schlake, T., and Dietz-Pfeilstetter, A. (1996) Scaffold/matrix-attached regions: Topological switches with multiple regulatory functions. Crit. Rev. Eukaryot. Gene Expr. **6**,115–138

Bratzel, F., López-Torrejón, G., Koch, M., Del Pozo, J. C., and Calonje, M. (2010) Keeping cell identity in *Arabidopsis* requires PRC1 RING-finger homologs that catalyze H2A monoubiquitination. Curr Biol **20**, 1853–1859

Cai S, Han HJ, Kohwi-Shigematsu T. (2003) Tissue-specific nuclear architecture and gene expression regulated by SATB1. Nat Genet. **34**, 42-51

Cao, Y., Dai Y., Cui, S., and Ma, L. (2008) Histone H2B monoubiquitination in the chromatin of *FLOWERING LOCUS C* regulates flowering time in *Arabidopsis*. Plant Cell **20**, 2566–2602

Castillejo, C., and Pelaz, S. (2008) The balance between CONSTANS and TEMPRANILLO activities determines *FT* expression to trigger flowering. Curr. Biol. **18**, 1338–1343

Cerdán P. D., and Chory, J. (2003) Regulation of flowering time by light quality. Nature **423**, 881–885

Choi, K., Kim, J., Hwang, H. J., Kim, S., Park, C., Kim, S. Y., and Lee, I. (2011) The FRIGIDA complex activates transcription of *FLC*, a strong flowering repressor in *Arabidopsis*, by recruiting chromatin modification factors. Plant Cell **23**, 289–303

Coupland, G., and Prat Monguio, S. (2005) Cell signalling and gene regulation signalling mechanisms in plants: Examples from the present and the future. Curr. Opin. Plant Biol. **8**, 457–461

Deal, R. B., Kandasamy, M. K., McKinney, E. C., and Meagher, R. B. (2005) The nuclear actin-related protein ARP6 is a pleiotropic developmental regulator required for the maintenance of *FLOWERING LOCUS C* expression and repression of flowering in *Arabidopsis*. Plant Cell **17**, 2633–2646

Ehrenhofer-Murray AE. (2004) Chromatin dynamics at DNA replication, transcription and repair. Eur. J. Biochem. **271**, 2335–2349

Farrona, S., Coupland, G., and Turck, F. (2008) The impact of chromatin regulation on the floral transition. Cell Dev. Biol. **19**, 560-573

Farrona, S., Hurtado, L., March-Diaz, R., Schmitz, R. J., Florencio, F. J., Turck, F., Amasino, R. M., and Reyes, J. C. (2011) Brahma is required for proper expression of the floral repressor FLC in *Arabidopsis*. PLoS One **6**, e17997

Finnegan, E. J., and Dennis, E. S. (2007) Vernalization-induced trimethylation of histone H3 lysine 27 at FLC is not maintained in mitotically quiescent cells. Curr. Biol. **17**, 1978-1983

Fujimoto, S., Matsunaga, S., Yonemura, M., Uchiyama, S., Azuma, T., and Fukui, K. (2004) Identification of a novel plant MAR DNA-binding protein localized on chromosomal surfaces. Plant Mol. Biol. **56**, 225–239

Greb T, Mylne JS, Crevillen P, Geraldo N, An H, Gendall AR, and Dean C. (2007) The PHD finger protein VRN5 functions in the epigenetic silencing of *Arabidopsis* FLC. Curr. Biol. **17**, 73–78

Gu X, Jiang D, Wang Y, Bachmair A, and He Y. (2009) Repression of the floral transition via histone H2B monoubiquitination. Plant J. **57**, 522–533

Han, H. J., Russo, J., Kohwi, Y., and Kohwi-Shigematsu, T. (2008) SATB1 reprogrammes gene expression to pro-mote breast tumour growth and metastasis. Nature **452**, 187-193

He, Y. (2009) Control of the transition to flowering by chromatin modifications Mol. Plant **2**, 554–564

He, Y. (2012) Chromatin regulation of flowering. Trends Plant Sci. **17**, 556–562

He, Y., Michaels, S. D., and Amasino, R. M. (2003) Regulation of flowering time by histone acetylation in *Arabidopsis*. Science **302**, 1751–1754

Hepworth, S. R., Valverde, F., Ravenscroft, D., Mouradov, A., and Coupland, G. (2002) Antagonistic regulation of flowering-time gene *SOC1* by CONSTANS and FLC via seperate promoter motifs. EMBO J. **21**, 4327–4337

Hollender, C., and Liu, Z. (2008) Histone deacetylase genes in *Arabidopsis* development. J. Integr. Plant Biol. **50**, 875–885

Hong, S. Y., Kim, O. K., Kim, S. G., Yang, M. S., and Park, C. M. (2011) Nuclear import and DNA binding of the ZHD5 transcription factor is modulated by a competitive peptide inhibitor in *Arabidopsis*. J. Biol. Chem. **286**, 1659–1668

Jeong, J. H., Song, H. R., Ko, J. H., Jeong, Y. M., Kwon, Y. E., Seol, J. H., Amasino, R. M., Noh, B., and Noh, Y. S. (2009) Repression of *FLOWERING LOCUS T* chromatin by functionally redundant histone H3 lysine 4 demethylases in *Arabidopsis*. PLoS ONE **4**, e8033.

Jiang D, Yang W, He Y, and Amasino RM (2007) *Arabidopsis* relatives of the human lysine-specific Demethylase1 repress the expression of *FWA* and *FLOWERING LOCUS C* and thus promote the floral transition. Plant Cell **19**, 2975–2987

Jiang, D., Wang, Y., Wang, Y., and He, Y. (2008) Repression of *FLOWERING LOCUS C* and *FLOWERING LOCUS T* by the *Arabidopsis* polycomb repressive complex 2 components. PLoS One **3**, e3404

Jones-Rhoades, M. W., Bartel, D. P., and Bartel, B. (2006) MicroRNAS and their regulatory roles in plants. Annu. Rev. Plant Biol. **57**, 19–53

Kardailsky, I., Shukla, V.K., Ahn, J.H., Dagenais, N., Christensen, S.K., Nguyen, J.T., Chory, J., Harrison, M.J., and Weigel, D. (1999) Activation tagging of the floral inducer *FT*. Science **286**, 1962–1965

Kim, Y. S., Kim, S. G., Park, J. E., Park, H. Y., Lim, M. H., Chua, N. H., and Park, C. M. (2006) A membrane-bound NAC transcription factor regulates cell division in *Arabidopsis*. Plant Cell **18**, 3132–3144

Kirmizis, A., Bartley, S. M., Kuzmichev, A., Margueron, R., Reinberg, D., Green, R., and Farnham, P. J. (2004) Silencing of human polycomb target genes is associated with methylation of histone H3K27. Genes Dev. **18**, 1592–1605

Kobayashi, Y., Kaya, H., Goto, K., Iwabuchi, M., and Araki, T. (1999) A pair of related genes with antagonistic roles in mediating flowering signals. Science **286**, 1960–1962

Kornberg, R. D. (1974) Chromatin structure: A repeating unit of histones and DNA. Science **184**, 868–871

Kumar, P. P., Purbey, P. K., Ravi, D. S., Mitra, D., and Galande, S. (2005) Displacement of SATB1-bound histone deacetylase 1 corepressor by the human immunodeficiency virus type 1 transactivator induces expression of interleukin-2 and its receptor in T cells. Mol. Cell Biol. **25**, 1620–1633

Kumar, S. V., and Wigge, P. A. (2010) H2A.Z-containing nucleosomes mediate the thermosensory response in *Arabidopsis*. Cell **140**, 136–147

Kumar, S. V., Lucyshyn, D., Jaeger, K. E., Alós, E., Alvey, E., Harberd, N. P., and Wigge P. A. (2012) Transcription factor PIF4 controls the thermosensory activation of flowering. Nature **484**, 242–245

Lee, H., Suh, S. S., Park, E., Cho, E., Ahn, J. H., Kim, S. G., Lee, J. S., Kwon, Y. M., and Lee, I. (2000) The AGAMOUS-LIKE 20 MADS domain protein integrates floral inductive pathways in *Arabidopsis*. Genes Dev. **14**, 2366–2376

Lim, P. O., Kim, Y., Breeze, E., Koo, J. C., Woo H. R., and Ryu J. S. (2007) Overexpression of a chromatin architecture-controlling AT-hook protein extends leaf longevity and increases the post-harvest storage life of plants. Plant J. **52**, 1140–1153

Litt, M. D., Simpson, M., Gaszner, M., Allis, C. D., and Felsenfeld, G. (2001) Correlation between histone lysine methylation and developmental changes at the chicken β-globin locus. Science **293**, 2453–2455

Liu, F., Marquardt, S., Lister, C., Swiezewski, S., and Dean, C. (2010) Targeted 3' processing of antisense transcripts triggers *Arabidopsis FLC* chromatin silencing. Science **327**, 94–97

Liu, F., Quesada, V., Crevillen, P., Baurle, I., Swiezewski, S., and Dean, C. (2007b) The *Arabidopsis* RNA-binding protein FCA requires a lysine-specific demethylase 1 homolog to downregulate *FLC*. Mol. Cell **28**, 398–407

Liu, J., He, Y., Amasino, R., and Chen, X. (2004). siRNAs targeting an intronic transposon in the regulation of natural flowering behavior in *Arabidopsis*. Genes Dev. **18**, 2873–2878

Lu, F., Cui, X., Zhang, S., Jenuwein, T., and Cao, X. (2011) *Arabidopsis* REF6 is a histone H3 lysine 27 demethylase. Nat. Genet. **43**,715-719

Lu, F., Cui, X., Zhang, S., Liu, C., and Cao, X. (2010) JMJ14 is an H3K4 demethylase regulating flowering time in *Arabidopsi*s. Cell Res. **20**, 387–390

Lu, H., Zou, Y., and Feng, N. (2010) Overexpression of *AHL20* negatively regulates defenses in *Arabidopsis*. J. Integr. Plant Biol. **52**, 801–808

Matsushita, A., Furumoto, T., Ishida, S., and Takahashi, Y. (2007) AGF1, an AT-hook protein, is necessary for the negative feedback of AtGA3ox1 encoding GA 3-oxidase. Plant Physiol. **143**, 1152–1162

Metcalf, C. E., and Wassarman, D. A. (2006) DNA binding properties of TAF1 isoforms with two AT-hooks. J. Biol. Chem. **281**, 30015–30023

Michaels, S. D., and Amasino, R. M. (1999) *FLOWERING LOCUS C* encodes a novel MADS domain protein that acts as a repressor of flowering. Plant Cell **11**, 949–956

Mizoguchi, T. and Coupland, G. (2000) ZEITLUPE and FKF1: novel connections between flowering time and circadian clock control. Trends in Plant Science **5**, 409–411

Mizoguchi, T., Wright, L., Fujiwara, S., Cremer, F., Lee, K., Onouchi, H., Mouradov, A., Fowler, S., Kamada, H., Putterill, J. and Coupland, G. (2005) Distinct roles of GIGANTEA in promoting flowering and regulating circadian rhythms in *Arabidopsis*. Plant Cell **17**, 2255–2270

Moon, Y. H., Chen, L., Pan, R. L., Chang, H. S., Zhu, T., Maffeo, D. M., and Sung, Z. R. (2003) *EMF* genes maintain vegetative developmentby repressing the flower program in *Arabidopsis*. Plant Cell **15**, 681–693

Mouradov, A., Cremer, F. and Coupland, G. (2002) Control of flowering time : Interacting pathways as a basis for diversity. Plant Cell **14**, S111–S130

Ng, K. H., Yu, H., and Ito, T. (2009) AGAMOUS controls *GIANT KILLER*, a multifunctional chromatin modifier in reproductive organ patterning and differentiation. PLoS Biol. **7**, e1000251

Parviz F., Hall D. D., Markwardt D. D., and Heideman W. (1998) Transcriptional regulation of *CLN3* expression by glucose in Saccharomyces cerevisiae. J. Bacteriol. **180**, 4508–4515

Pederson, T. (2000) Half a century of "the nuclear matrix. Mol. Biol. Cell **11**, 799–805

Pien, S., Fleury, D., Mylne, J. S., Crevillen, P., Inzé, D., Avramova, Z., Dean, C., and Grossniklausa, U. (2008) *ARABIDOPSIS* TRITHORAX1 dynamically regulates *FLOWERING LOCUS C* activation via histone H3 lysine-4 trimethylation. Plant Cell **20**, 580–588

Piñeiro, M., Gómez-Mena, C., Schaffer, R, Martínez-Zapater, J.M. and Coupland, G. (2003) EARLY BOLTING IN SHORT DAYS is related to chromatin remodeling factors and regulates flowering in *Arabidopsis* by repressing *FT*. Plant Cell **15**, 1552−1562

Purbey, P. K., Singh, S., Notani, D., Kumar, P. P., Limaye, A. S., and Galande, S. (2009) Acetylation-dependent interaction of SATB1 and CtBP1 mediates transcriptional repression by SATB1. Mol. Cell Biol. **29**, 1321–1337

Reeves, P. H., and Coupland, G. (2001) Analysis of flowering time control in *Arabidopsis* by comparison of double and triple mutants. Plant Physiology **126**, 1085–1091

Reeves, R. (2001) Molecular biology of HMGA proteins: hubs of nuclear function. Gene **277**, 63–81

Reeves, R. (2010) nuclear functions of the HMG proteins. Biochim. Biophys. Acta **1799**, 3–14

Reeves, R., and Nissen, M. S. (1990) The A·T-DNA-binding domain of mammalian high mobility group I chromosomal proteins. J. Biol. Chem. **265**, 8573-8582

Rudd, S., Frisch, M., Grote, K., Meyers, B. C., Mayer, K., and Werner, T. (2004) Genome-wide in silico mapping of scaffold/matrix attachment regions in *Arabidopsis* suggests correlation of intragenic scaffold/matrix attachment regions with gene expression. Plant Physiol. **135**, 715–722

Samach, A., and Coupland, G. (2000) Time measurement and the control of flowering in plants. BioEssays **22**, 38–47

Samach, A., and Wigge, P.A.(2005) Ambient temperature perception in plants. Curr. Opin. Plant Biol. **8**, 483–486

Samach, A., Onouchi, H., Gold, S. E., Ditta, G. S., Schwarz-Sommer, Z., Yanofsky, M. F., and Coupland, G. (2000) Distinct roles of CONSTANS target genes in reproductive development of *Arabidopsis*. Science **288**, 1613–1616

Santos-Rosa, H., Schneider, R., Bannister, A. J., Sherriff, J., Bernstein, B. E., Emre, N. C., Schreiber, S. L., Mellor, J., and Kouzarides, T. (2002) Active genes are trimethylated at K4 of histone H3. Nature **419**, 407–411

Schena, M., and Davis, R. W. (1992) HD-Zip proteins, members of an *Arabidopsis* homeodomain protein superfamily. Proc. Natl. Acad. Sci. U.S.A. **89**, 3894–3898

Schmitz, R.J., Sung, S., and Amasino, R.M. (2008) Histone arginine methylation is required for vernalization-induced epigenetic silencing of *FLC* in winter-annual *Arabidopsis thaliana*. PNAS **105**, 411–416.

Schneider, R., and Grosschedl, R. (2007) Dynamics and interplay of nuclear architecture, genome organization and gene expression. Genes Dev. **21**, 3027–3043

Searle, I., and Coupland, G. (2004) Induction of flowering by seasonal changes in photoperiod. EMBO J. **23**, 1217–1222

Searle, I., He, Y., Turck, F., Vincent, C., Fornara, F., Kröber, S., Amasino, R. A., and Coupland, G. (2006) The transcription factor FLC confers a flowering response to vernalization be repressing meristem competence and systemic signaling in *Arabidopsis*. Genes Dev. **20**, 898–912

Sessa, G., Morelli, G., and Ruberti, I. (1993) The Athb-1 and -2 HD-Zip domains homodimerize forming complexes of different DNA binding specificities. EMBO J. **12**, 3507–3517

Silverstein, R. A., Richardson, W., Levin, H., Allshire, R., and Ekwall, K. (2003) A new role for the transcriptional corepressor SIN3; regulation of centromeres. Curr. Biol. **13**, 68–72

Simon, R., and Coupland, G. (1996) *Arabidopsis* genes that regulate flowering time in response to day-length. Semin. Cell Dev. Biol. **7**, 419–425

Simpson, G. G. (2004) The autonomous pathway. Epigenetic and post-transcriptional gene regulation in the control of *Arabidopsis* flowering time. Curr. Opin. Plant Biol. **7**, 570–574

Simpson, G. G., and Dean, C. (2002) *Arabidopsis*, the Rosetta stone of flowering time? Science **296**, 285–289

Simpson, G. G., Dijkwel, P. P., Quesada, V., Henderson, I., and Dean, C. (2003) FY is an RNA 3′-end processing factor that interacts with FCA to control the *Arabidopsis* floral transition. Cell **13**, 777–787

Street, I. H., Shah, P. K., Smith, A. M., Avery, N., and Neff, M. M. (2008) The AT-hook-containing proteins SOB3/AHL29 and ESC/AHL27 are negative modulators of hypocotyl growth in *Arabidopsis*. Plant J. **54**, 1–14

Suárez-López, P., Wheatley, K., Robson, F., Onouchi, H., Valverde, F. and Coupland, G. (2001) CONSTANS mediates between the circadian clock and control of flowering in *Arabidopsis*. Nature **410**, 1116-1120.

Sung S., and Amasino R. M. (2004) Vernalization and epigenetics: How plants remember winter. Curr. Opin. Plant Biol. **7**, 4–10

Sung, S., and Amasino, R. M. (2004) Vernalization in *Arabidopsis thaliana* is mediated by the PHD finger protein VIN3. Nature **427**, 159–164

Sung, S., Schmitz, R.J., and Amasino, R.M. (2006) A PHD finger protein involved in both the vernalization and photoperiod pathways in *Arabidopsis*. Genes Dev. **20**, 3244–3248.

Swiezewski, S., Crevillen, P., Liu, F., Ecker, J.R., Jerzmanowski, A., and Dean, C. (2007) Small RNA-mediated chromatin silencing directed to the 3' region of the *Arabidopsi*s gene encoding the developmental regulator, FLC. Proc. Natl. Acad. Sci. USA **104**, 3633–3638

Takada, S., and Goto, K. (2003) *TERMINAL FLOWER 2*, an *Arabidopsis* homolog of *HETEROCHROMATIN PROTEIN1*, counteracts the activation of *FLOWERING LOCUS T* by *CONSTANS* in the vascular tissues of leaves to regulate flowering time. Plant Cell **15**, 2856–2865

Tetko, I. V., Haberer, G., Rudd, S., Meyers, B., Mewes, H. W., and Mayer, K. F. (2006) Spatiotemporal expression control correlates with intragenic scaffold matrix attachment regions (S/MARs) in *Arabidopsis thaliana*. PLoS Comput. Biol. **2**, e21

Thomashow, M. F. (2001) So what's new in the field of plant cold acclimation? Lots! Plant Physiol. **125**, 89–93

Turck, F., Fornara, F., and Coupland, G. (2008) Regulation and identity of florigen: Flowering Locus T moves center stage. Annu. Rev. Plant Biol. **59**, 573–594

Turck, F., Roudier, F., Farrona, S., Martin-Magniette, M. L., Guillaume, E., Buisine, N., Gagnot, S., Martienssen, R. A., Coupland, G., and Colot, V. (2007) *Arabidopsis* TFL2/LHP1 specifically associates with genes marked by trimethylation of histone H3 lysine27. PLoS Genet **3**, e86

Vinson, C., Acharya, A., and Taparowsky, E. J. (2006) Deciphering B-ZIP transcription factor interactions in vitro and in vivo. Biochim. Biophys. Acta **1759**, 4–12

Vom Endt, D., Soares e Silva, M., Kijne, J. W., Pasquali, G., and Memelink, J. (2007) Identification of a bipartite jasmonate-responsive promoter element in the Catharanthus roseus ORCA3 transcription factor gene that interacts specifically with AT-hook DNA-binding proteins. Plant Physiol.**144**, 1680-1689

Wang, T. Y., Han, Z. M., Chai, Y. R., and Zhang, J. H. (2010) A minireview of MAR-binding proteins. Mol. Biol. Rep. **37**, 3553–3560

Wang, X., Zhang, Y., Ma, Q., Zhang, Z., Xue, Y., Bao, S., and Chong, K. (2007) SKB1-mediated symmetric dimethylation of histone H4R3 controls flowering time in *Arabidopsis*. EMBO J. **26**, 1934–1941.

Weigel, D., Ahn, J. H., Blázquez, M. A., Borevitz, J. O., Christensen, S. K., Fankhauser, C., Ferrandiz, C., Kardailsky, I., Malancharuvil, E. J., Neff, M. M., Nguyen, J. T., Sato, S., Wang, Z. Y., Xia, Y., Dixon, R. A., Harrison, M. J., Lamb, C. J., Yanofsky, M. F., and Chory, J. (2000) Activation tagging in *Arabidopsis*. Plant Physiol. **122**, 1003–1013

Wigge, P. A., Kim, M. C., Jaeger, K. E., Busch, W., Schmid, M., Lohmann, J. U., and Weigel, D. (2005) Integration of spatial and temporal information during floral induction in *Arabidopsis*. Science **309**, 1056–1059

Xiao, C., Chen, F., Yu, X., Lin, C., and Fu, Y. F. (2009) Overexpression of an AT-hook gene, AHL22, delays flowering and inhibits the elongation of the hypocotyl in *Arabidopsis thaliana*. Plant Mol. Biol. **71**, 39–50

Yaish, M. W., Colasanti, J., and Rothstein, S. J. (2011) The role of epigenetic processes in controlling flowering time in plants exposed to stress. J. Exp. Bot. **62**, 3727–3735

Yang, S. D., Seo, P. J., Yoon, H. K., and Park, C. M. (2011) The *Arabidopsis* NAC transcription factor VNI2 integrates abscisic acid signals into leaf senescence via the COR/RD genes. Plant Cell **23**, 2155–2168

Yang, W., Jiang, D., Jiang, J., He, Y. (2010) A plant-specific histone H3 lysine 4 demethylase represses the floral transition in *Arabidopsis*. Plant J. **62**, 663–673

Yanovsky, M. J., and Kay, S. A. (2002) Molecular basis of seasonal time measurement in *Arabidopsis*. Nature **419**, 308–312

Yasui, D., Miyano, M., Cai S. T., Varga-Weisz, P., and Kohwi-Shigematsu, T. (2002) SATB1 targets chromatin remodel-ling to regulate genes over long distances. Nature; **419**, 641–645

Yoo, S. D., Cho, Y. H., and Sheen, J. (2007) *Arabidopsis* mesophyll protoplasts. A versatile cell system for transient gene expression analysis. Nat. Protoc. **2**, 1565–1572

Zilberman, D., Coleman-Derr, D., Ballinger, T., and Henikoff, S. (2008) Histone H2A.Z and DNA methylation are mutually antagonistic chromatin marks. Nature **456**, 125–129

VII. PUBLICATION LIST

Bold First Author

1. Jae-Hoon Jung, ***Ju Yun***, Yeon-Hee Seo and Chung-Mo Park. (2005) Characterization of an Arabidopsis gene that mediates cytokinin signaling in shoot apical meristem development. Molecular Cells 19, 342-349.

2. Jung-Eun Park, Ju-young Park, Youn-sung Kim, Paul E.Staswick, Jin Jeon, ***Ju Yun***, Sun-Young Kim, Junmook Kim, Yong-Hwan Lee and Chung-mo Park (2007) GH3-Mediated Auxin Homeostasis Links Growth Regulation with Stess Adaptation Response in Arabidopsis. Journal of biological chemistry 282, 10036-10046.

3. Jae-Hoon Jung, Yeon-Hee Seo, Pil Joon Seo, Jose Luis Reyes, ***Ju Yun***, Nam-Hai Chua and Chung-Mo Prak (2007) The GIGANTEA-regulated microRNA172 mediates photoperiodic flowering independent of CONSTANS in Arabidopsis. Plant Cell 19, 2736-2748.

4. **[Ju Yun, Sang-Gyu Kim], Shinyoung Hong and Chung-Mo Park (2008) (short communication) Small interfering peptides as a novel way of transcriptional control. Plant Signaling & Behavior 3, 1-3.**

5. Jae-Hoon Jung, *Ju Yun*, Pil Joon Seo, Jae-Hyung Lee and Chung-Mo Park (2012) The SOC1-SPL module integrates photoperiod and gibberellic acid signals to control flowering time in Arabidopsis. Plant journal 69,577-588.

6. Ju Yun, Youn-Sung Kim, Jae-Hoon Jung, Pil Joon Seo and Chung-Mo Park (2012) The AT-Hook Motif-Containing Protein AHL22 Regulates Flowering Initiation by Modifying FLOWERING LOCUS T chromatin in Arabidopsis. Journal of Biological Chemistry 287, 15307-15316.

7. Jae-Hoon Jung, Sangmin Lee, *Ju Yun*, MinYoung Lee and Chung-Mo Park (2014) The miR172 target TOE3 represses AGAMOUS expression during Arabidopsis floral patterning. Plant Science 215–216, 29–38

VIII. ABSTRACT IN KOREAN (국문 초록)

개화의 체계적인 조화는 발달 상태와 계절적인 신호들과 함께 식물에 있어서 번식의 성공에 중요하다. 개화시기가 변화된 애기장대 돌연변이체에서의 분자유전학적 연구들은 다른 유전학적 개화 경로들에 속한 다수의 유전자들을 밝혀왔다. 개화 시기 조절 유전자들은 RNA 대사와 염색질 변형들과 같은 다양한 분자적, 생화학적 기작들에 의해 조절된다. 최근 연구들에서는 AT-hook DNA-binding motif 를 포함한 단백질들은 식물의 발달단계와 스트레스 반응들에 관여하는 것으로 알려져 있다.

본 연구를 통해 AT-hook protein AHL22 (AT-hook motif nuclear localized 22)가 *FLOWERING LOCUS T* (*FT*) 염색질을 변형시켜서 개화시기를 조절한다는 것을 증명하였다. 또한 AHL22 와 *FT* 유전자가 잎의 관다발 조직(vascular tissues)에서 같이 발현되며, 발달과정 동안 AHL22 가 *FT* 발현을 억제하는 것을 관찰하였다. AHL22 단백질은 *FT* 유전자내의 AT-rich sequence 에 결합한다. 또한 일부 Histone deacetylase 들과도 결합한다.

애기장대 *AHL22* 유전자의 과량발현 돌연변이체 (OE-*AHL22*)는 개화가 늦어지고, *FT* 발현이 상당히 감소되어 있다. OE-*AHL22* 돌연변이체에서 개화의 지연과 *FT* 감소와 일치하여, *FT* 크로마틴에서 히스톤 3 아세틸화가 감소된 반면, 히스톤 3 라이신 9 디메틸화는 증가되었다. 본 연구는 AHL22 단백질이 히스톤 3 아세틸화와 메틸화를 조절함으로써 *FT* 크로마틴의 구조를 변경시키는 크로마틴 재배치 인자로 작용한다는 것을 제안한다.

핵심어: 애기장대 · 개화시기 · AT-hook DNA binding protein · AT-rich sequence · FT · **크로마틴**

학번: 2003-30870